

# **A New Multi-Model Absolute Difference-based Sensitivity (MMADS) Analysis Method to Screen Non-influential Processes under Process Model and Parametric Uncertainty**

Jing Yang<sup>1,2</sup> and Ming Ye<sup>2</sup>

<sup>1</sup>College of Water Resources and Architectural Engineering, Northwest A&F University, Yangling 712100, Shaanxi, China

<sup>2</sup>Department of Earth, Ocean, and Atmosphere Science and Department of Scientific Computing, Florida State University, Tallahassee, FL 32306, USA.

Corresponding author: Ming Ye ([mye@fsu.edu](mailto:mye@fsu.edu))

Jing Yang (ORCID ID: 0000-0001-9838-5102)

Ming Ye (ORCID ID: 0000-0002-7080-0578)

Revision submitted for publication in Journal of Hydrology

February 2022

Page 1

## **Highlights**

- A new sensitivity analysis method called MMADS is developed.
- MMADS extends Morris method from parameter space to parameter-model space.
- MMADS addresses uncertainty in both process model structures and model parameters.

## Abstract

1  
2 Process-based models have been widely used for hydrologic modeling, and it is a common  
3 practice to use sensitivity analysis methods for excluding non-influential hydrologic processes  
4 from further investigation and/or model improvement. This study develops a new method called  
5 multi-model absolute difference-based sensitivity (MMADS) analysis method to screen non-  
6 influential system processes and parameters. MMADS is conceptually similar to the Morris  
7 method for addressing parametric uncertainty, but has a unique feature to address both process  
8 model uncertainty (i.e., a process may be represented by multiple process models) and process  
9 model parameter uncertainty (i.e., parameters associated with a process model are random).  
10 MMADS first evaluates absolute differences of a quantity of interest (i.e., a system model  
11 output) by varying process models and/or process model parameter values, and then calculates  
12 the mean and variance of the differences for investigating process influence. The mean measures  
13 overall influence of the process on the quantity of interest, and the variance estimates influence  
14 of nonlinear effects of the process and/or its interactions with other processes. MMADS is an  
15 extension of the Morris method from a parameter space to a joint parameter-model space for  
16 explicitly addressing both process model uncertainty and model parameter uncertainty. The  
17 performance of MMADS is evaluated by using two numerical experiments. One experiment is  
18 based on Sobol's  $G^*$ -function with ten product elements, and has analytical solutions of the  
19 MMADS mean and variance of absolute differences. The other experiment is for groundwater  
20 flow modeling which considers three processes (i.e., recharge, geology, and snowmelt) that  
21 interact with each other. Results indicate that MMADS is computationally efficient and can  
22 identify non-influential processes of complex hydrological systems.

23 **Keywords:** Model uncertainty, Process sensitivity, Non-influential process, Morris method

## 24 1. Introduction

25 Process-based hydrological modeling has been widely used over the last couple of decades  
26 for understanding and predicting behaviors of hydrological and environmental systems (Clark et  
27 al., 2015a, 2015b; Gorelick and Zheng, 2015; Singh, 2018). These systems are often open and  
28 complex, and involve a number of processes and process interactions (Brenner et al., 2018; Clark  
29 et al., 2015c). Beven (2002) noted that “*the development of more and more complex models that*  
30 *incorporate more and more detail about processes, but which introduce more and more*  
31 *parameters that must be calibrated, does not appear to be the future*”. It is also unnecessary to  
32 include all system processes and process interactions, because it happens often that only a subset  
33 of processes exerts a strong influence on system behaviors. It is a common practice in hydrologic  
34 and environmental modeling to first identify non-influential processes and process interactions,  
35 and then to exclude them from model development and/or improvement (e.g., Singh, 2018; Zeng  
36 et al., 2018; Ciric et al., 2012; Ketema and Langergraber, 2015). This is called *Factor Fixing*  
37 setting by Saltelli et al. (2004; 2008) in a statistical context. Sensitivity analysis has long been  
38 used for factor fixing setting to identify non-influential model parameters by investigating  
39 relations between model parameters and model outputs (Becker et al., 2018; Devak and Dhanya,  
40 2017; Huo et al., 2019; Haan, 1989; Pianosi et al., 2016; Song et al., 2015; Sobol’ et al., 2007;  
41 Razavi and Gupta, 2015; Razavi et al., 2021). This concept can be extended to identify non-  
42 influential process based on the idea that a process is considered to be non-influential if model  
43 parameters associated with the process are identified as non-influential (Markstrom et al. 2016;  
44 Sheikholeslami et al. 2021). A widely used method of parameter sensitivity analysis method is  
45 the derivative-based Morris screening method (Morris, 1991). Although the Morris method is  
46 theoretically less rigorous and practically less quantitative than Sobol’s variance-based methods

47 (Wainwright et al., 2014; Feng et al., 2019), it is conceptually straightforward and  
48 computationally efficient for screening non-influential parameters. This study uses the design  
49 ideas of the Morris screening method, but extends the ideas to consider not only parametric  
50 uncertainty but also process model uncertainty.

51 Consider a hydrological system composed of two interacting processes  $A$  and  $B$  as shown in  
52 Fig. 1. In the conventional way of developing a system model to represent the system, as shown  
53 in Fig. 1, a system process (or a process for brevity) is represented by a single process model.  
54 For example, process  $A$  is represented by process model  $M_A(\boldsymbol{\theta}_A)$ , where  $M_A$  denotes the process  
55 model and  $\boldsymbol{\theta}_A$  is the model parameter, a vector of multiple parameters that are always treated as  
56 random variables. Integrating these process models gives a single system model  $M$ . This concept  
57 of single-model representation of a system and its processes (and process interactions) has  
58 become questionable when process model uncertainty arises, i.e., available data and knowledge  
59 support multiple process models to represent a process, e.g., process model  $M_A^1(\boldsymbol{\theta}_A^1)$  and  
60  $M_A^2(\boldsymbol{\theta}_A^2)$  for process  $A$ , as illustrated in Fig. 1. In a modular modeling framework to form a  
61 system model by integrating process models, process model uncertainty leads to system model  
62 uncertainty, i.e., multiple alternative system models ( $M_1, M_2, \dots$ ) are all plausible. An example of  
63 this is given in Fig. 3 of Clark et al. (2015a) that introduced the structure for unifying multiple  
64 modeling alternative (SUMMA) approach. Other examples of surface water and groundwater  
65 modeling are given in Clark et al. (2008), Ye et al. (2010; 2016), Lu et al. (2015), Elshall and  
66 Tsai (2014), Chitsazan and Tsai (2014), and Haghnegahdar et al. (2017). Since modeled system  
67 behaviors depend on the choice of process models, influence of a process on a system output  
68 (e.g., hydraulic head) is likely to be different when the process is simulated by different process

69 models. Without considering process model uncertainty and only considering parametric  
70 uncertainty, identification of non-influential process may lead to biased results.

71 This study tackled the following question: *can we correctly screen out non-influential*  
72 *processes if we are not certain about the choice of process models and model parameters?* A key  
73 to answering this question is how to consider model uncertainty for identifying non-influential  
74 processes. Hydrologic model uncertainty has been studied for about two decades (Beven, 2002;  
75 Bredehoeft, 2003, 2005; Neuman, 2003; Poeter and Anderson, 2005), and there has been a  
76 number of studies on investigating influence of a process under multiple system models (Herman  
77 et al., 2013; Baroni and Tarantola, 2014; Savage et al., 2016; Dai and Ye, 2015; Dai et al.,  
78 2017a, 2017b, 2019; Mai et al., 2020; Dell'Oca et al., 2020). All these methods are  
79 computationally expensive, as they require Monte Carlo simulations in a parameter space to  
80 approximate variance (or other statistical moments) of a quantity of interest. Although  
81 computational cost can be reduced by various approaches (see the review article of Razavi et al.,  
82 2021), a large number of model executions are still needed.

83 This problem of high computational cost may be avoided if one is only interested in  
84 screening out non-influential processes rather than ranking system processes. Based on Morris'  
85 one-factor-at-a-time concept, Van Hoey et al. (2014) developed a method to vary model  
86 components one at a time. A model component was defined by Van Hoey et al. (2014) as "*a*  
87 *conceptual description of a subprocess of the entire model*", which appears to be equivalent to a  
88 system process that is of interest to this study. The method of Van Hoey et al. (2014) applied the  
89 method to multiple alternative models of a process for evaluating the mean of absolute  
90 elementary effects, denoted as  $\mu^*$ , an important term of the Morris method as discussed in  
91 Section 2.1. The  $\mu^*$  values of any two alternative process models are plotted in a so-called

92 “*evaluation chart*”, and the chart is used to evaluate impacts of process models on model outputs  
93 or model evaluation metrics. While this method is conceptually straightforward and easy to  
94 implement, it performs sensitivity analysis on individual system models, and does not explicitly  
95 consider impacts of process models on model outputs, because the method does not evaluate  
96 variation of model outputs caused by changing from one process model to another process  
97 model. In other words, the method of Van Hoey et al. (2014) is still for a parameter space within  
98 a single system model, but not for a joint parameter-model space across multiple system models.

99 The goal of this study is thus to develop a new method, called multi-model absolute  
100 difference-based sensitivity (MMADS) analysis method, which expands the design ideas of  
101 Morris screening method from a parameter space to a joint parameter-model space. MMADS  
102 evaluates not only the differences of a model output due to varying model parameter values but  
103 also the differences due to varying process models. After the differences are evaluated for each  
104 process, their mean and variance are calculated and used to identify non-influential processes.  
105 The calculation of mean and variance in the model space is based on model averaging methods  
106 that have been used in the hydrologic community for several decades (Beven, 2002; Neuman,  
107 2003; Ye et al., 2004; Poeter and Anderson, 2005). A process with both small mean and small  
108 variance is considered to be non-influential. A small mean indicates small differences of model  
109 output when changing process models and process model parameter values. A small variance is  
110 resulted from a lack of nonlinear effects and/or interactions between process models and/or  
111 process model parameter values. Similar to the Morris screening method, the MMADS method is  
112 computationally efficient, and this makes MMADS appealing to real-world applications for  
113 identifying non-influential processes. Two numerical examples are employed to evaluate  
114 performance of MMADS. One example is based on a Sobol’s  $G^*$ -function with ten product

115 elements (each element representing a process), and has analytical expressions for the mean and  
 116 variance of MMADS. The other example is for groundwater flow modeling with three  
 117 interacting processes related to recharge, geology, and snowmelt. Robustness of MMADS,  
 118 effects of process model weights, and limitations of MMADS are also discussed in paper.

119

## 120 **2. Background, Definitions, and Conceptualization**

### 121 **2.1. Morris Screening Method for Parameters of a Single Model**

122 To better understand the rationale of developing the MMADS method, we start by briefly  
 123 revisiting the Morris screening method for addressing parametric uncertainty of a single system  
 124 model (Morris, 1991). Following Saltelli et al. (2004), we use  $y(\mathbf{x})$  to denote a model output  
 125 evaluated with  $k$  parameters,  $\mathbf{x} = (x_1, x_2, \dots, x_k)$ . The range of each parameter is scaled (e.g., by  
 126 using its cumulative distribution) to the unit interval  $[0, 1]$ , and the unit interval is then  
 127 partitioned into  $(p-1)$  equally sized intervals, where  $p$  represents the number of levels. The  
 128 Morris screening method evaluates the elementary effect ( $EE$ ) via

$$129 \quad EE_i = \frac{[y(x_1, \dots, x_{i-1}, x_i + \delta, x_{i+1}, \dots, x_k) - y(\mathbf{x})]}{\delta},$$

130 (1)

131 where  $EE_i$  is the elementary effect of the  $i$ -th parameter  $x_i$ ;  $\delta$  is a predetermined multiple of the  
 132 interval with the size of  $1/(p-1)$ ;  $\mathbf{x} = (x_1, \dots, x_{i-1}, x_i, x_{i+1}, \dots, x_k)$  is the vector of the reference  
 133 parameter values, and each value is selected randomly from the set  $\{0, 1/(p-1), 2/(p-1), \dots, 1\}$   
 134 except  $x_i$  from the set  $\{0, 1/(p-1), 1/(p-1), \dots, 1-\delta\}$  so that  $(x_i + \delta)$  is still in range of  $[0, 1]$ .  
 135 Randomly sampling  $x_i$  gives a number of  $EE_i$ , and three statistics of  $EE_i$  are computed: the mean  
 136 ( $\mu_i$ ) of  $EE_i$ , the mean ( $\mu_i^*$ ) of absolute  $EE_i$ , and the standard deviation ( $\sigma_i$ ) of  $EE_i$ . As noted by

137 Campolongo et al. (2007),  $\mu^*$  is a better choice than  $\mu$  for detecting parameters that have  
138 important overall influence on the output, because  $\mu^*$  avoids canceling out  $EE$  values with  
139 opposite signs. The standard deviation,  $\sigma_i$ , is used to detect parameters that either have nonlinear  
140 effects on the output or interact with other parameters to affect the output. A parameter with  
141 small  $\mu^*$  and  $\sigma$  values is identified as non-influential. Since the Morris screening method is  
142 qualitative in nature in comparison with other global sensitivity analysis methods such as Sobol's  
143 variance-based methods, it is commonly used for screening non-influential parameters, rather  
144 than quantitatively ranking importance or influence of model parameters.

145 Fig. 2(a) is an illustration of evaluating the  $EE$  values based on a figure of Saltelli et al.  
146 (2004). For the purpose of illustration, we assume that the system has two processes, denoted as  
147  $A$  and  $B$ , and that each process is represented by one process model, i.e.,  $M_A$  for process  $A$  and  
148  $M_B$  for process  $B$ . We further assume that each process model has only one parameter, i.e.,  $x_A$  for  
149  $M_A$  and  $x_B$  for  $M_B$ . The system model is thus denoted as  $M_A(x_A) \cup M_B(x_B)$  by integrating  
150 process models  $M_A$  and  $M_B$ . With the number of levels  $p = 5$  and  $\delta = 1/4$ , a total of 20  $EE$  values  
151 are obtained for each parameter, i.e., the 20 black solid arrows for  $x_A$  and the 20 black dashed  
152 arrows for  $x_B$ , as shown in Fig.2(a). If all the 20  $EE$  values are small and the variation of the 20  
153  $EE$  values is also small, the corresponding  $\mu^*$  and  $\sigma$  values are small. This indicates that the  
154 model output changes slightly when parameter values change, and the parameter is non-  
155 influential. A process is identified to be non-influential if its model parameters are identified to  
156 be non-influential by the Morris screening method. If a process model contains more than one  
157 parameter, the Morris screening method can be applied to a group of parameters associated with  
158 the process (Saltelli et al., 2004).

## 159 **2.2. Basic Ideas of MMADS Method**

160 Fig. 2(b) illustrates the design ideas of MMADS to consider both process model uncertainty  
161 and parametric uncertainty. In line with Fig. 2(a), we still assume that the system has two  
162 processes,  $A$  and  $B$ . To consider process model uncertainty, we assume that process  $A$  can be  
163 represented by two alternative process models,  $M_A^1$  and  $M_A^2$ . An example of this is the Penman-  
164 Monteith method (Monteith, 1995) and the Hargreaves method (Hargreaves et al., 1985) for  
165 estimating potential evapotranspiration. For the sake of illustration in Fig. 2(b), we assume that  
166 each process model has only one parameter, i.e., parameters  $x_A^1$  and  $x_A^2$  for  $M_A^1$  and  $M_A^2$ ,  
167 respectively. Similarly, process  $B$  also has two alternative process models, i.e., process model  
168  $M_B^1$  with parameter  $x_B^1$  and process model  $M_B^2$  with parameter  $x_B^2$ . As a result, we have four  
169 system models denoted as  $M_A^1(x_A^1) \cup M_B^1(x_B^1)$ ,  $M_A^1(x_A^1) \cup M_B^2(x_B^2)$ ,  $M_A^2(x_A^2) \cup M_B^1(x_B^1)$ , and  
170  $M_A^2(x_A^2) \cup M_B^2(x_B^2)$ . It should be noted that the simple example of Fig. 2(b) with two processes  
171 and one parameter for each process is only for illustrating the design ideas of MMADS.  
172 MMADS is applicable to a real-world system that contains more than two processes, each of  
173 which has more than one parameter.

174 To illustrate the MMADS design ideas, we first assume that parametric uncertainty does not  
175 exist, i.e., the true values of the parameters  $x_A^1$ ,  $x_A^2$ ,  $x_B^1$ , and  $x_B^2$  are known. In this case, MMADS  
176 evaluates the absolute difference,  $d\Delta$ , of the system model output,  $\Delta$ , in the following two  
177 situations under process model uncertainty:

- 178 (1) Transition between the two process models of process  $A$ , conditioning on model  $M_B^1$  of  
179 process  $B$ . The term “transition” is used here to represent the change within a process model  
180 or from one process model to another process model. In our case, there are four transitions  
181 between the two models of process  $A$  as follows:

182  $T_{M_A} = \{M_A^1 \rightarrow M_A^1, M_A^1 \rightarrow M_A^2, M_A^2 \rightarrow M_A^1, M_A^2 \rightarrow M_A^2\}$ , where  $T_{M_A}$  denote the set of process  
183 model transitions of process  $A$  and the symbol “ $\rightarrow$ ” denotes the transition. The absolute  
184 difference,  $d\Delta$ , of model output for each transition is evaluated, and then averaged over all  
185 the four transitions to yield  $E_{T_{M_A}}(d\Delta|M_B^1)$  (the way of calculating the average is discussed  
186 below). The  $E_{T_{M_A}}(d\Delta|M_B^1)$  term is conditioned on  $M_B^1$ , and measures how the changes  
187 between and within the two process models  $M_A = \{M_A^1, M_A^2\}$  of process  $A$  affect system  
188 model output given process model  $M_B^1$ . Since there is no parametric uncertainty at this stage,  
189  $d\Delta = 0$  for  $M_A^1 \rightarrow M_A^1$  and  $M_A^2 \rightarrow M_A^2$ , and  $d\Delta$  for  $M_A^1 \rightarrow M_A^2$  equals  $d\Delta$  for  $M_A^2 \rightarrow M_A^1$ .  
190 These however are not the case when parametric uncertainty exists for the process models,  
191 and more discussion on this is given later.

192 (2) Transition between the two models of process  $A$ , conditioning on model  $M_B^2$  of process  $B$ .  
193 Repeating the calculation above for  $M_B^2$ , we have  $E_{T_{M_A}}(d\Delta|M_B^2)$  that is conditioned on  $M_B^2$ ,  
194 and measures how the changes between and within the two process models,  $M_A = \{M_A^1, M_A^2\}$ ,  
195 affect system model output given  $M_B^2$ .

196 For the two terms  $E_{T_{M_A}}(d\Delta|M_B^1)$  and  $E_{T_{M_A}}(d\Delta|M_B^2)$  obtained in steps (1) and (2), we calculate  
197 the average  $E_A(d\Delta) = E_{M_B} E_{T_{M_A}}(d\Delta|M_B)$  for process  $A$ , which measures how the changes  
198 between and within the two models of process  $A$  affect the system model output. Similarly, we  
199 can also have  $E_B(d\Delta) = E_{M_A} E_{T_{M_B}}(d\Delta|M_A)$  for process  $B$ , which measures how the changes  
200 between and within the two models of process  $B$  affect system model output. If process  $A$  is more  
201 influential than process  $B$  to the system model output, then  $E_A(d\Delta)$  should be larger than

202  $E_B(d\Delta)$ . The calculation for the average,  $E(d\Delta)$ , of  $d\Delta$  can be extended to a calculation for the  
 203 variance,  $V(d\Delta)$ , of  $d\Delta$ , and its corresponding equation is given in Section 3.

204 Now let us consider parametric uncertainty, i.e., true parameter values are unknown but  
 205 parameter probability distributions are known. In this case, we use  $\mathbf{x}$  to denote a set of parameter  
 206 values; the true parameter value,  $x$ , may be viewed as one realization of the random parameter.  
 207 As shown in Fig. 2(b), each parameter range is discretized into  $(p-1)$  equally sized intervals.  
 208 With the parametric uncertainty,  $d\Delta \neq 0$  for transition  $M_A^1 \rightarrow M_A^1$ , because the transition means  
 209 changes from one point of  $\mathbf{x}_A^1$  to another point of  $\mathbf{x}_A^1$ . This parameter transition is denoted as  
 210  $x_A^1 \rightarrow x_A^{1'}$ , where  $x_A^1$  and  $x_A^{1'}$  are two points of  $\mathbf{x}_A^1$ . In this case,  $d\Delta$  may be denoted as  
 211  $d\Delta | (x_B, M_B, M_A^1 \rightarrow M_A^1, x_A^1 \rightarrow x_A^{1'})$ , which reads as the difference of a system model output for  
 212 the parameter transition  $x_A^1 \rightarrow x_A^{1'}$  associated with process model transition  $M_A^1 \rightarrow M_A^1$   
 213 conditioning on parameter value  $x_B$  (one parameter realization from  $\mathbf{x}_B^1$  or  $\mathbf{x}_B^2$ ) of process model  
 214  $M_B$  ( $M_B^1$  or  $M_B^2$ ) for process  $B$ . Similarly, we can obtain the  $d\Delta$  values for the other three  
 215 process model transitions in  $T_{M_A}$ .

216 For each of the four process model transitions in  $T_{M_A}$ , there are multiple parameter  
 217 transitions due to parametric uncertainty, resulting in multiple  $d\Delta$  values for a single process  
 218 model transition. We calculate the average of  $d\Delta$  first over the parameter transitions within a  
 219 process model transition and then across the process model transitions conditioning on a specific  
 220 point  $x_B$  of process model  $M_B$ . This gives  $E_{T_{M_A}}(d\Delta | x_B, M_B) = E_{T_{M_A}} E_{T_{x_A} | T_{M_A}}(d\Delta | x_B, M_B, T_{x_A}, T_{M_A})$ ,  
 221 where  $T_{x_A}$  denotes a parameter transition of  $\mathbf{x}_A$  for the process model transition  $T_{M_A}$  of process  $A$ .

222 We further take average first over all parameter points ( $\mathbf{x}_B$ ) and then over all process models ( $\mathbf{M}_B$ )  
223 of process  $B$ . This gives  
224  $E_A(d\Delta) = E_{\mathbf{M}_B} E_{T_{M_A}} (d\Delta | M_B) = E_{\mathbf{M}_B} E_{\mathbf{x}_B | M_B} E_{T_{M_A}} E_{T_{x_A} | T_{M_A}} (d\Delta | x_B, M_B, T_{x_A}, T_{M_A})$  for process  $A$ . The  
225  $E_B(d\Delta)$  term for process  $B$  can be evaluated in the same way. The variance,  $V(d\Delta)$ , of  $d\Delta$  for  
226 process  $A$  can be evaluated in a similar way, and a general equation is given in Section 3.  
227  $E_A(d\Delta)$ ,  $E_B(d\Delta)$ ,  $V_A(d\Delta)$ , and  $V_B(d\Delta)$  are the most critical quantities of MMADS, and they  
228 consider both process model uncertainty and model parameter uncertainty.

229 Fig. 2(b) illustrates the transitions between process models and between process model  
230 parameters. Figs. 2(b1) and 2(b2) (the top row of Fig. 2(b)) shows the transitions conditioning on  
231 parameter  $x_B^1$  of process model  $M_B^1$ . The red arrows in Fig. 2(b1) represent possible parameter  
232 transitions  $x_A^1 \rightarrow x_A^1$  for process model transition  $M_A^1 \rightarrow M_A^1$ , and the blue arrows in Fig. 2(b2)  
233 represent possible parameter transitions  $x_A^2 \rightarrow x_A^2$  for process model transition  $M_A^2 \rightarrow M_A^2$ . The  
234 black arrows from Fig. 2(b1) to Fig 2(b2) illustrate possible parameter transition  $x_A^1 \rightarrow x_A^2$  for  
235 process model transition  $M_A^1 \rightarrow M_A^2$ , and the green arrows from Fig. 2(b2) to Fig 2(b1) illustrate  
236 possible parameter transitions  $x_A^2 \rightarrow x_A^1$  for process model transition  $M_A^2 \rightarrow M_A^1$ . Similarly, Figs.  
237 2(b1) and 2(b2) (the bottom row of Fig. 2(b)) show the transitions conditioning on parameter  $x_B^2$   
238 of process model  $M_B^2$ . Because different process models may have different numbers of  
239 parameters and the parameters may have different physical meanings and ranges, MMADS does  
240 not use the derivative-based  $EE$  of the Morris method, but uses the absolute difference,  $d\Delta$ , of  
241 model output  $\Delta$ .

242

### 243 3. Mathematical Formulation and Numerical Implementation

#### 244 3.1 Mathematical Formulation

245 The basic ideas explained above are generalized in this section for any number of system  
246 processes and any number of process models of each process. We first define mathematical  
247 symbols used in the generalization. If process model uncertainty and parametric uncertainty do  
248 not exist, system variable,  $\Delta = M(\theta) = M(\theta_1, \dots, \theta_d)$ , is simulated by a single system model,  $M$ ,  
249 with a vector of  $d$ -dimensional system model parameters,  $\theta = \{\theta_1, \dots, \theta_d\}$ . Note that we here use  $\theta$   
250 to denote a set of deterministic parameter values, and reserve  $\Theta$  to denote a set of random  
251 parameter values ( $\theta$  can be viewed as a realization of  $\Theta$ ). If the system of interest consists of  
252 multiple processes (denoted as  $A, B, \dots$ ) and each process has its own process model (denoted as  
253  $M_A, M_B, \dots$ ) and associated parameters (denoted as  $\theta_A, \theta_B, \dots$ ), the system model,  $M(\theta)$ , may be  
254 viewed as an integration of the process models, i.e.,  $M(\theta) = \cup(M_A(\theta_A), M_B(\theta_B), \dots)$ , together  
255 with other system model components common to the processes (e.g., domain discretization,  
256 system initial conditions, and driving forces). The process model integration (denoted by the  
257 union symbol above) may need to consider nonlinear interactions between the process models.  
258 An example of such an integration was given in Dai et al. (2019) for developing a system model  
259 of groundwater reactive transport by integrating processes of groundwater flow, thermal  
260 transport, solute transport, and biogeochemical reactions. In addition, a process may have its sub-  
261 processes. For example, a groundwater flow process may consist of sub-processes such as  
262 recharge, geology, and evapotranspiration. More discussions on process-based modular modeling  
263 are referred to Clark et al. (2008, 2015a, 2015b, 2016).

264 With the presence of process model uncertainty, a system process may be represented by  
265 several alternative process models. Taking process  $A$  as an example, it may be represented by

266 multiple process models that form a set,  $\mathbf{M}_A(\theta_A) = \{M_A^1(\theta_A^1), M_A^2(\theta_A^2), \dots\}$ ; each process model  
 267 may have its own parameters or share parameters with other process models. Integration of the  
 268 alternative process models leads to alternative system models, i.e.,  
 269  $\mathbf{M}(\theta) = \cup(\mathbf{M}_A(\theta_A), \mathbf{M}_B(\theta_B), \dots)$ . If the process model parameters are random, they are denoted as  
 270  $\boldsymbol{\theta}$  to be differentiated from  $\theta$ , which is viewed as a realization of  $\boldsymbol{\theta}$ . In this case,  
 271  $\mathbf{M}(\theta) = \cup(\mathbf{M}_A(\theta_A), \mathbf{M}_B(\theta_B), \dots)$  becomes  $\mathbf{M}(\boldsymbol{\theta}) = \cup(\mathbf{M}_A(\boldsymbol{\theta}_A), \mathbf{M}_B(\boldsymbol{\theta}_B), \dots)$ .

272 We first give the equations of mean and variance of  $d\Delta$  for process  $K$  (e.g., process  $A$  in  
 273 Section 2.2) with a consideration of process model uncertainty only. Following the definition of  
 274 posterior mean and variance of Bayesian model averaging (e.g., Eqs. (4) and (5) in Ye et al.  
 275 (2004)), the mean and variance of  $d\Delta$  for process  $K$  are defined as

$$276 E_K(d\Delta) = E_{\mathbf{M}_{\sim K}} E_{T_{\mathbf{M}_K}}(d\Delta | M_{\sim K}) \quad ,$$

277 (2)

$$278 V_K(d\Delta) = E_{\mathbf{M}_{\sim K}} V_{T_{\mathbf{M}_K}}(d\Delta | M_{\sim K}) + V_{\mathbf{M}_{\sim K}} E_{T_{\mathbf{M}_K}}(d\Delta | M_{\sim K}) \quad ,$$

279 (3)

280 where  $\mathbf{M}_{\sim K}$  in the subscription is the set of multiple process model combinations that represent  
 281 all processes but  $K$  ( $\sim K$ , e.g., process  $B$  in Section 2.2),  $\mathbf{M}_K$  is the set of multiple process models  
 282 only for process  $K$ , and  $T_{\mathbf{M}_K}$  is the set of process model transitions within process  $K$ , i.e.,  
 283  $T_{\mathbf{M}_K} = \{M_K^i \rightarrow M_K^j\}$  where  $i, j=1, 2, \dots, N_{M_K}$  with  $N_{M_K}$  being the number of process models  
 284 that represent process  $K$ .

285 Eq. (2) indicates that, if model output,  $\Delta$ , changes substantially when a process'  
 286 representation changes from  $M_K^i$  to  $M_K^j$ , then this process is considered to have significant

287 influence on the model output. Since there are multiple process model transitions for process  $K$ ,  
 288 it is practically sensible to use the average  $E_{T_{M_K}}(d\Delta | M_{\sim K})$  of  $d\Delta$  over all possible transitions. In  
 289 addition, since the average for process  $K$  is for a combination,  $M_{\sim K}$ , of the process models for  
 290 all the processes but process  $K$ , it is necessary to evaluate the average,  $E_{\mathbf{M}_{\sim K}} E_{T_{M_K}}(d\Delta | M_{\sim K})$ ,  
 291 over all the combinations. The mean,  $E_K(d\Delta)$ , of the output difference for process  $K$  thus  
 292 measures the overall influence of process  $K$  through the transitions between any two process  
 293 models.

294 The variance,  $V_K(d\Delta)$ , of the output difference defined in Eq. (3) measures to what extent  
 295 the output difference spreads out due to nonlinear effects of the process models and/or  
 296 interaction effects between process  $K$  and other processes. The nonlinear effect is reflected by  
 297 the  $V_{T_{M_K}}(d\Delta | M_{\sim K})$  term, in that, if the process models are nonlinear,  $d\Delta$  is large for a transition  
 298 from one process model to another process model. The  $E_{\mathbf{M}_{\sim K}} V_{T_{M_K}}(d\Delta | M_{\sim K})$  term measures the  
 299 average nonlinear effect over model set  $\mathbf{M}_{\sim K}$ . The interaction effect is reflected in the  
 300  $V_{\mathbf{M}_{\sim K}} E_{T_{M_K}}(d\Delta | M_{\sim K})$  term, in that the variance  $V_{\mathbf{M}_{\sim K}}$  is large when  $E_{T_{M_K}}(d\Delta | M_{\sim K})$  is evaluated  
 301 for two models in model set  $\mathbf{M}_{\sim K}$ , i.e.,  $M_K$  of process  $K$  interacting with  $M_{\sim K}$  of all process but  $K$ .

302 Eqs. (2) and (3) can be extended to address parameters of the process models, and the  
 303 detailed derivation for the extension is given in Appendix A. The extended Eqs. (2) and (3) are

$$304 \quad E_K(d\Delta) = E_{\mathbf{M}_{\sim K}} E_{\theta_{\sim K} | M_{\sim K}} E_{T_{M_K}} E_{T_{\theta_K} | T_{M_K}}(d\Delta | \theta_{\sim K}, M_{\sim K}, T_{\theta_K}, T_{M_K}), \quad (4)$$

$$305 \quad V_K(d\Delta | K) = E_{\mathbf{M}_{\sim K}} E_{\theta_{\sim K} | M_{\sim K}} E_{T_{M_K}} E_{T_{\theta_K} | T_{M_K}}(d\Delta | \theta_{\sim K}, M_{\sim K}, T_{\theta_K}, T_{M_K})^2$$

$$- \left( E_{\mathbf{M}_{\sim K}} E_{\theta_{\sim K} | M_{\sim K}} E_{T_{M_K}} E_{T_{\theta_K} | T_{M_K}}(d\Delta | \theta_{\sim K}, M_{\sim K}, T_{\theta_K}, T_{M_K}) \right)^2,$$

$$306 \quad (5)$$

307 where subscript  $\theta_{\sim K} | M_{\sim K}$  of  $E_{\theta_{\sim K} | M_{\sim K}}$  indicates that the expectation is with respect to random  
308 parameter  $\theta_{\sim K}$  specific to model  $M_{\sim K}$ , and subscript  $T_{\theta_K} | T_{M_K}$  of  $E_{T_{\theta_K} | T_{M_K}}$  indicates that the  
309 expectation is with respect to the random parameters involved in the parameter transitions,  $T_{\theta_K}$ ,  
310 associated with the process model transitions  $T_{M_K}$ . The  $\theta_{\sim K}$  and  $T_{\theta_K}$  terms in the parentheses are  
311 a single realization of  $\theta_{\sim K}$  and  $T_{\theta_K}$ , respectively. Taking the process model transition  
312  $T_{M_K} = \{M_A^1 \rightarrow M_A^2\}$  as an example, the set of parameter transitions with respect to  $M_A^1 \rightarrow M_A^2$  is  
313  $T_{\theta_A} = \{\theta_A^{1(m)} \rightarrow \theta_A^{2(n)}\}$ , where  $\theta_A^{1(m)}$  and  $\theta_A^{2(n)}$  are two randomly selected parameter realizations in  
314  $\theta_A^1$  and  $\theta_A^2$ .  $T_{\theta_A}$  includes all possible parameter transitions from parameters of  $M_A^1$  to  
315 parameters of  $M_A^2$ . When process model uncertainty does not exist (i.e., each process is  
316 represented by only one process model), Eqs. (4) and (5) become

$$317 \quad E_K(d\Delta) = E_{\theta_{\sim K}} E_{T_{\theta_K}} (d\Delta | \theta_{\sim K}, T_{\theta_K}) \quad ,$$

318 (6)

$$319 \quad V_K(d\Delta) = E_{\theta_{\sim K}} E_{T_{\theta_K}} (d\Delta | \theta_{\sim K}, T_{\theta_K})^2 - \left( E_{\theta_{\sim K}} E_{T_{\theta_K}} (d\Delta | \theta_{\sim K}, T_{\theta_K}) \right)^2 \quad .$$

320 (7)

321 These are similar to the mean and variance of elementary effects in the Morris screening method,  
322 and can be used to screen non-influential parameters for a single system model.

323 For either a single or multiple system models,  $E_K(d\Delta)$  and  $V_K(d\Delta)$  are used in the same way  
324 as that the mean and standard deviation ( $\mu^*$  and  $\sigma$ ) of  $EE$  are used. The  $E_K(d\Delta)$  and  $V_K(d\Delta)$  of all  
325 processes under consideration are plotted in a 2-D plane, and a process is more influential than  
326 other processes if its  $E_K(d\Delta)$  and  $V_K(d\Delta)$  values are larger than those of other processes.  
327 However, we do not suggest using MMADS to rank processes or identify influential processes,

328 but to screen non-influential processes, because the MMADS method is qualitative in nature for  
 329 process identification. A quantitative process ranking can be done by using more rigorous (but  
 330 more computationally expensive) approaches such as the first-order process sensitivity index  
 331 developed by Dai et al. (2017a).

332

### 333 3.2. Model Averaging and Monte Carlo Integration

334 The expectations with respect to the process models ( $E_{M_{-K}}$ ) and process model transitions ( $E_{T_{M_K}}$ ) in Eqs. (4) and (5) can be evaluated using the model averaging method via

$$336 E_{M_{-K}} E_{\theta_{-K}|M_{-K}}(\square) = \sum E_{\theta_{-K}|M_{-K}}(\square) P(M_{-K}), \quad (8)$$

$$338 E_{T_{M_K}} E_{T_{\theta_K}|T_{M_K}}(\square) = \sum E_{T_{\theta_K}|T_{M_K}}(\square) P(T_{M_K}), \quad (9)$$

340 where the dot ( $\bullet$ ) denotes the quantities in Eqs. (4) and (5) (e.g.,  
 341  $E_{T_{M_K}} E_{T_{\theta_K}|T_{M_K}}(d\Delta|\theta_{-K}, M_{-K}, T_{\theta_K}, T_{M_K})$  in Eq. (4)),  $P(M_{-K})$  is the probability (model averaging  
 342 weight) of a combination of the models for all the processes but process  $K$ ,  $P(T_{M_K})$  is the  
 343 probability of the transition from one process model to another process model.

344 Evaluating  $P(M_{-K})$  and  $P(T_{M_K})$  requires that the probability,  $P(M_K)$ , of process models for  
 345 process  $K$  satisfy  $\sum P(M_K) = 1$ . To evaluate  $P(M_{-K})$  for a combination of process models, it is  
 346 assumed that selecting one process model of a process is independent to selecting one process  
 347 model of another process. With this assumption,  $P(M_{-K})$  can be evaluated as

$$348 P(M_{-K}) = \prod_{i=1}^{N_{-K}} P(M_{-K,i}), \text{ where } N_{-K} \text{ equals the number of processes minus one (i.e., the number}$$

349 of all processes but process  $K$ ) and  $P(M_{\sim K,i})$  is the probability of a process model  $M_{\sim K,i}$ .  
 350 Taking a system with three processes  $A$ ,  $B$ , and  $C$  as an example, each process has two alternative  
 351 models (i.e.,  $A_1, A_2, B_1, B_2, C_1$ , and  $C_2$ ), and the process models have the following probabilities,  
 352 i.e.,  $P(A_1) = P(A_2) = 0.5$ ,  $P(B_1) = 0.7$ ,  $P(B_2) = 0.3$ ,  $P(C_1) = 0.6$ , and  $P(C_2) = 0.4$ . The  
 353 combination,  $B_1C_1$ , of process models  $B_1$  and  $C_1$  has the probability of  $P(B_1C_1) = 0.7 \times 0.6 =$   
 354  $0.42$ .  $P(T_{M_K})$  of the process model transition  $M_K^i \rightarrow M_K^j$  can be evaluated as  
 355  $P(T_{M_K}) = P(M_K^i) \times P(M_K^j)$ , where  $P(M_K^i)$  and  $P(M_K^j)$  are the process model probabilities of  
 356  $M_K^i$  and  $M_K^j$ , respectively. This calculation implies that each process model transitions has its  
 357 own probability, depending on the probabilities of the two process models of the transition.  
 358 Using process  $B$  and its process model probabilities in the example above, the probability for  
 359 transition  $M_B^1 \rightarrow M_B^1$  is 0.49, and the probability for the transition  $M_B^1 \rightarrow M_B^2$  is 0.21. The  
 360 process model probabilities can be either prior probability determined based on prior information  
 361 or posterior probability determined by using both prior information and observations used for  
 362 model calibration and uncertainty quantification. Prior probabilities are used in this study, and  
 363 evaluating posterior probabilities with Bayesian model averaging is discussed in Dai et al.  
 364 (2017a) and Lu et al. (2015).

365 The expectations ( $E_{\theta_{\sim K}|M_{\sim K}}(\square)$  and  $E_{T_{\theta_K}|T_{M_K}}(\square)$ ) with respect to the process model parameters  
 366 and parameter transitions can be evaluated using Monte Carlo methods. For the convenience of  
 367 discussion, we use the same number,  $n$ , of parameter realizations for each process model  
 368 combination  $M_{\sim K}$  and process model  $M_K$ . To evaluate the mean and variance of  $d\Delta$  using Eqs.  
 369 (4) and (5), a total  $(N_{M_{\sim K}} \times n) \times (N_{M_K}^2 \times n^2)$  numbers of  $d\Delta$  are needed, where  $N_{M_K}$  and  $N_{M_{\sim K}}$   
 370 are the number of models of process  $K$  and the number of combinations of the models for all

371 processes but  $K$ , respectively; the square terms are for the parameter transitions and process  
372 model transitions. To obtain  $(N_{M_{-K}} \times n) \times (N_{M_K}^2 \times n^2)$  numbers of  $d\Delta$  requires a total  
373  $(N_{M_{-K}} \times n) \times (N_{M_K} \times n)$  numbers of model executions. To reduce computational cost, the  $n$   
374 parameter realizations can be generated using the Latin Hypercube Sampling (LHS) method, so  
375 that a small number of realizations can cover the entire parameter space. The procedure of  
376 generating the realizations of  $\theta_{-K} | M_{-K}$  and  $\theta_K | M_K$  and the procedure of computing  
377  $d\Delta | (\theta_K, M_K, \theta_{-K}, M_{-K})$  and  $d\Delta | (\theta_{-K}, M_{-K}, T_{\theta_K}, T_{M_K})$  are as follows:

378 **Step 1:** Divide the cumulative distribution of each parameter into  $n$  equal strata, and sample  $n$   
379 parameter values from the  $n$  strata using the LHS method. This results in a sample matrix  
380 with the dimension of  $n \times n_p$ , where  $n_p$  is the total number of parameters involved in the  
381 multi-models.

382 **Step 2:** For each process model combination  $M_{-K}$ , combine the columns of parameter values  
383 (from the parameter matrix generated in Step 1) for parameters associated with  $M_{-K}$  to  
384 yield the parameter set  $\theta_{-K} | M_{-K}$ .

385 **Step 3:** For each process model  $M_K$ , combine the columns of parameter values (from the  
386 parameter matrix generated in Step 1) for parameters associated with  $M_K$  to yield the  
387 parameter set  $\theta_K | M_K$ .

388 **Step 4:** Loop over the parameter sets  $\theta_{-K} | M_{-K}$  and  $\theta_K | M_K$ , compute  $\Delta | (\theta_K, M_K, \theta_{-K}, M_{-K})$ .

389 **Step 5:** Loop over the process model transitions and parameter transitions to compute  
390  $d\Delta | (\theta_{-K}, M_{-K}, T_{\theta_K}, T_{M_K})$ .

391 Fig. 3 shows the pseudo code to compute the mean and variance of  $d\Delta$  based on Eqs. (4) and (5)  
392 and the parameter sampling procedure described above.

393

#### 394 **4. Two Numerical Experiments**

395 MMADS is evaluated using two numerical experiments. One experiment is based on the  
396 Sobol's  $G^*$ -function, which is commonly used as a benchmark function for sensitivity analysis  
397 (Saltelli et al., 2010). Since mean  $E_K(d\Delta)$  and variance  $V_K(d\Delta)$  can be analytically derived, this  
398 experiment can be used to verify the computer code based on the pseudo code shown in Fig. 3.  
399 The other numerical experiment is for one-dimensional groundwater flow modeling based on the  
400 synthetic case developed by Dai et al. (2017a). The two examples demonstrate the capability and  
401 efficiency of MMADS for screening non-influential processes under both parametric uncertainty  
402 and process model uncertainty.

#### 403 **4.1. Sobol's $G^*$ -function**

404 The Sobol's  $G^*$ -function is defined as (Saltelli et al., 2010):

$$405 \quad G^*(X_1, \dots, X_k; a_1, \dots, a_k; \delta_1, \dots, \delta_k; \alpha_1, \dots, \alpha_k) = \prod_{i=1}^k g_i^* \quad (10)$$
$$g_i^* = \frac{(1 + \alpha_i) \cdot |2(X_i + \delta_i) - I[X_i + \delta_i] - 1|^{\alpha_i} + a_i}{1 + a_i}$$

406 where  $X_i$  is a parameter following uniform distribution  $U[0, 1]$ ,  $a_i \in \mathbb{R}^+$  is a positive coefficient,  
407  $\delta_i \in [0, 1]$  and  $\alpha_i > 0$  are shift and curvature parameters, respectively, and  $I[X_i + \delta_i]$  is the  
408 integer part of  $X_i + \delta_i$ . The analytical solutions of the first-order ( $S_i$ ) and total-effect ( $S_{Ti}$ )  
409 sensitivity indices for parameter  $X_i$  were given by Saltelli et al. (2010) as

$$410 \quad S_i = V_i / V \quad \text{and} \quad S_{Ti} = V_{Ti} / V \quad , \quad \text{where} \quad V_i = \frac{\alpha_i^2}{(1 + 2\alpha_i)(1 + a_i)^2} \quad , \quad V_{Ti} = V_i \prod_{j \neq i} (1 + V_j) \quad , \quad \text{and}$$

411  $V = \prod_{i=1}^k (1 + V_i) - 1$ . The total-effect sensitivity index,  $S_{Ti}$ , is of particular importance to this study

412 because it can quantitatively measure influence of  $X_i$  on the  $G^*$ -function. The  $S_{T_i}$ -based ranking  
 413 of parameter influence is used as a reference to evaluate whether MMADS can identify non-  
 414 influential parameters for a single system model. For example, if a parameter is identified to be  
 415 non-influential by  $S_{T_i}$ , it should also be identified by MMADS as non-influential. The influence  
 416 of  $X_i$  is controlled by the curvature parameter  $\alpha_i$  and coefficient  $a_i$ . A larger  $\alpha_i$  and a smaller  
 417  $a_i$  give a larger total-effect parameter sensitivity index  $S_{T_i}$ , indicating higher influence of  $X_i$ .  
 418 Since  $S_{T_i}$  does not depend on the shift parameter,  $\delta_i$ , we set  $\delta_i = 0$  in this study. The  $g_i^*$   
 419 function in Eq. (10) is then simplified to

$$420 \quad g_i^* = \frac{(1 + \alpha_i) \cdot |2X_i - 1|^{\alpha_i} + a_i}{1 + a_i} .$$

421 (11)

#### 422 **4.1.1. Processes and Process Models**

423 For an illustrative purpose, we set  $k = 10$  in Eq. (10) to consider ten product elements,  $g_i^*$   
 424 ( $i=1, 2, \dots, 10$ ), and assume that each element  $g_i^*$  represents a process. When there is no process  
 425 model uncertainty, Eqs. (6) and (7) derived for parameter sensitivity analysis are used for  
 426 identify non-influential processes. Since each element has only one parameter  $X_i$ , the sensitivity  
 427 of parameter  $X_i$  is viewed as the sensitivity of process  $g_i^*$ . For example, if parameter  $X_1$  is the  
 428 least influential parameter among  $X_1 \sim X_{10}$ , then the process represented by  $g_1^*$  is the least  
 429 influential process among the ten processes represented by  $g_1^* \sim g_{10}^*$ .

430 To consider process model uncertainty, we assume that each  $g_i^*$  has two plausible process  
431 models,  $g_i^{*1}$  and  $g_i^{*2}$  ( $i = 1, 2, \dots, 10$ ), with the function form of Eq. (11) but different  $a_i$  and  $\alpha_i$   
432 values. The uniform distribution of parameter  $X_i$  is the same for the two process models. For the  
433  $\alpha$  values, we set  $\alpha_i^1 = 1$  and  $\alpha_i^2 = 2$  for all the ten processes, where the superscripts 1 and 2 are  
434 for the two process models. The  $a_i^1$  and  $a_i^2$  values of the ten processes are listed in Table 1, so  
435 that the process models are different with different levels of influence to model output. Taking  
436 the first process represented by  $g_1^*$  as an example, its two alternative process models are  
437  $g_1^{*1} = \frac{2|2X_1 - 1| + 0.002}{1.002}$  and  $g_1^{*2} = \frac{3|2X_1 - 1|^2 + 0.005}{1.005}$ . It should be noted that, although this  
438 experiment only considers ten processes, a combination of the process models yields a total of  
439  $2^{10} = 1,024$  system models. This large number of system models indicates that the numerical  
440 example with ten processes is complex enough for evaluating MMADS performance.

#### 441 4.1.2. Sensitivity Results for Individual System Models

442 Appendix B derives analytical expressions  $E_K(d\Delta)$  and  $V_K(d\Delta)$  of each process for a single  
443 system model of the Sobol's G\*-function. Since each process,  $g_i^*$ , has only one parameter,  $X_i$ ,  
444 the sensitivity of process  $g_i^*$  is reflected by the sensitivity of parameter  $X_i$ . Taking two system  
445 models,  $\prod_{i=1}^{10} g_i^{*1}$  and  $\prod_{i=1}^{10} g_i^{*2}$  as an example, Table 2 lists the analytical values of  $E_K(d\Delta)$  and  
446  $V_K(d\Delta)$  for parameters  $X_1 \sim X_{10}$  associated with the ten processes. Our numerical results are  
447 almost identical to the analytical results with the maximum relative error less than 3%. Table 2  
448 also lists the analytical results of Sobol's total-effect sensitivity index that is for estimating  
449 sensitivity of parameter  $X_i$ .

450 In MMADS, a process is considered to be less influential than other processes if its  $E_K(d\Delta)$   
451 and  $V_K(d\Delta)$  values are smaller than those of other processes. Taking system model  $\prod_{i=1}^{10} g_i^{*1}$  as an  
452 example, process  $g_{10}^*$  is the least influential process (or equivalently parameter  $X_{10}$  is the least  
453 influential parameter), because it has the smallest  $E_K(d\Delta)$  and  $V_K(d\Delta)$  values among the ten  
454 processes. The identification of the least influential process is consistent with the identification  
455 of the least influential parameter based on the Sobol's total-effect sensitivity index  $S_{Ti}$ . For  
456 system model  $\prod_{i=1}^{10} g_i^{*2}$ , the least influential process becomes  $g_9^*$ , which is also the case for  $S_{Ti}$ .  
457 The change of the least influential process is attributed to using different  $\alpha_i$  and  $a_i$  values for  
458 the two system models. The change happens to other system models, but results are not shown.  
459 Due to the changes, there is uncertainty in identifying non-influential system processes, and  
460 biased identification may be resulted if ignoring process model uncertainty. It is thus necessary  
461 to use MMADS for identifying non-influential process under process model uncertainty.

#### 462 4.1.3. Sensitivity Results for Multiple System Models

463 Based on Eqs. (4) and (5), Appendix C derives analytical expressions of  $E(d\Delta)$  and  $V(d\Delta)$  for  
464 multiple system models of the Sobol's  $G^*$ -function. To evaluate the  $E_K(d\Delta)$  and  $V_K(d\Delta)$  values,  
465 for each process, we assume that its two process models have equal weights, i.e.,  
466  $P(g_i^{*1}) = P(g_i^{*2}) = 0.5$ , and the analytical results of  $E_K(d\Delta)$  and  $V_K(d\Delta)$  are listed in Table 2. The  
467 numerical results are almost identical to the analytical results with the maximum relative error  
468 less than 3%. This verifies our computer codes based on the pseudo code shown in Fig. 3.

469 Fig. 4(a) illustrates how to use the  $E_K(d\Delta)$  and  $V_K(d\Delta)$  values for qualitatively identifying  
470 influential and non-influential processes for individual system models and multiple system

471 models. The  $E_K(d\Delta)$  and  $\sqrt{V_K(d\Delta)}$  values are plotted as cross symbols for the multiple system  
472 models and as open symbols for the individual system models. For the multiple system models,  
473 Fig. 4(a) suggests that  $g_1^*$  is the most influential process because it is located at the upper-right  
474 corner, and that  $g_9^*$  is the least influential process because it is located at the lower-left corner.  
475 For the 1,024 individual system models, the  $E_K(d\Delta)$  values of each process are separated into two  
476 groups with 512 models in each group. This is a special case for the Sobol-G\* function, because  
477 there are two process models for each process and the  $E_K(d\Delta)$  values of a process is determined  
478 only by the  $a$  and  $\alpha$  values of the process model as indicated by Eq. (B7).

479 MMADS should be used for identifying non-influential processes not for ranking process  
480 influence, because  $E_K(d\Delta)$  and  $V_K(d\Delta)$  are approximations. For example, Table 2 shows that, for  
481 the multiple system models, while  $E_K(d\Delta)$  of process  $g_4^*$  is slightly larger than that of  $g_5^*$ ,  
482  $V_K(d\Delta)$  of process  $g_4^*$  is smaller than that of  $g_5^*$ . It is thus difficult to rank the two processes.

## 483 **4.2. Groundwater Flow Modeling**

484 This numerical experiment of groundwater flow modeling is modified from Dai et al.  
485 (2017a). As shown in Fig. 5, the unconfined aquifer has the length of  $L=10,000$  m, which is  
486 under a steady state condition. The aquifer is bounded by two constant-head boundaries, and  
487 subject to a uniform precipitation. Process model uncertainty exists in the following three system  
488 processes: (1) recharge process that converts precipitation to aquifer recharge, (2) geology  
489 process that characterizes hydraulic conductivity of the aquifer, and (3) snowmelt process that  
490 estimates snow-melt rate to determine hydraulic head at the east boundary of the domain. The  
491 process models are described below.

### 492 **4.2.1. Processes and Process Models**

493 Following Dai et al. (2017a), two recharge models ( $R_1$  and  $R_2$ ) are used to simulate the  
 494 recharge process that converts precipitation [m/d] to groundwater recharge [m/d], and they are

$$495 \begin{aligned} R_1 : w &= a(P - 14)^{0.5} \\ R_2 : w &= b(P - 15.7) \end{aligned}$$

496 (12)

497 where  $a$  and  $b$  are scaling parameters [dimensionless] assumed to follow the normal distribution,  
 498  $N(2.0, 0.4^2)$ , and the uniform distribution,  $U(0.2, 0.5)$ , respectively,  $P$  is the annual precipitation  
 499 which is set as  $4.175 \times 10^{-3}$  m/d. Hydraulic conductivity ( $K$ ) [m/d] over the domain is  
 500 parameterized by two geology process models ( $G_1$  and  $G_2$ ) as follows,

$$501 \begin{aligned} G_1 : K & \text{ for any } x \\ G_2 : K & = \begin{cases} K_1 & \text{for } x < 7000 \\ K_2 & \text{for } x \geq 7000 \end{cases} \end{aligned}$$

502 (13)

503 In model  $G_1$ , the aquifer is assumed to be homogeneous, and the hydraulic conductivity follows  
 504 the lognormal distribution,  $LN(2.9, 0.5^2)$ . Model  $G_2$  has two zones of hydraulic conductivity  
 505 separated at the location of  $x_0 = 7,000$  m (Fig. 5). The hydraulic conductivities  $K_1$  of zone 1 ( $x <$   
 506  $7000$  m) and  $K_2$  of zone 2 ( $x \geq 7000$  m) are assumed to follow the lognormal distributions,  
 507  $LN(2.6, 0.3^2)$  and  $LN(3.2, 0.3^2)$ , respectively.

508 For the lake boundary, its hydraulic head is set to be constant at  $h_1 = 300$  m. For the river  
 509 boundary, the river stage,  $h_2$ , is determined by the empirical rating curve function below to  
 510 covert a river discharge into the river stage via

511  $h_2 = 0.3Q^{0.6} + 289$  ,

512 (14)

513 where  $Q$  is river discharge [ $\text{m}^3/\text{s}$ ], and the coefficients of 0.3, 0.6, and 289 are chosen arbitrarily  
 514 for this numerical experiment. The river discharge depends on snowmelt runoff via

515  $Q = C_{sn} \times M \times SVC \times A$  , (15)

516 where  $C_{sn}$  is runoff coefficient [dimensionless],  $M$  is snow-melt rate [ $\text{m}/\text{s}$ ],  $SVC$  is the ratio of  
 517 snow-covered area to watershed area,  $A$  [ $\text{m}^2$ ]. We arbitrarily set  $C_{sn} = 0.8$ ,  $SVC = 0.7$ , and  $A =$   
 518  $2,000 \text{ km}^2$ , and use two models to estimate the daily snow-melt rate, i.e., the degree-day method  
 519 and the restricted degree-day radiation balance method (Hock, 2003; Kustas et al., 1994;  
 520 Martinec et al., 2007). The two models are

521  $M_1 : M = f_1(T_a - T_m)$   
 522  $M_2 : M = f_2(T_a - T_m) + rR_n$  ,

522 (16)

523 where  $f_1$  and  $f_2$  are snowmelt factors [ $\text{mm}/(\text{°C} \cdot \text{d})$ ] that are assumed to follow normal  
 524 distributions,  $N(3.5, 0.75^2)$  and  $N(2.5, 0.3^2)$ , respectively,  $T_a$  [ $\text{°C}$ ] is the average temperature for  
 525 a given day, and  $T_m$  [ $\text{°C}$ ] is the temperature threshold (typically set to be 0) when snow melt  
 526 occurs. The second model considers the effects of surface radiation budget,  $R_n$  [ $\text{W}/\text{m}^2$ ], and uses  
 527 conversion factor  $r$  [ $(\text{mm}/\text{d})/(\text{W}/\text{m}^2)$ ] to convert the energy flux to snowmelt rate.  $T_a$  and  $R_n$  are  
 528 set as  $7 \text{ °C}$  and  $80 \text{ W}/\text{m}^2$ , respectively, and  $r$  is assumed to follow the normal distribution of  
 529  $N(0.3, 0.05^2)$ .

530 A combination of the two recharge process models, two geology process models, and two  
 531 snowmelt process models leads to a total of eight system models, and they are denoted as

532  $R_1G_1M_1, R_1G_1M_2, R_1G_2M_1, R_1G_2M_2, R_2G_1M_1, R_2G_1M_2, R_2G_2M_1,$  and  $R_2G_2M_2$ . All process models  
 533 have equal weights, i.e.,  $P(R_1) = P(R_2) = 0.5, P(G_1) = P(G_2) = 0.5,$  and  $P(M_1) = P(M_2) = 0.5$ . The  
 534 groundwater discharge per unit width at the location  $x_0 = 7,000$  m is the quantity of interest for  
 535 the sensitivity analysis, and it is labeled as  $q_0$  in Fig. 5. The analytical solution of the discharge,  
 536  $q(x)$ , at any location  $x$ , is derived as

$$537 \quad q(x) = K_1 \frac{h_1^2 - h_2^2}{2(x_0 - \lambda x_0 + \lambda L)} - \frac{1}{2} w \frac{x_0^2 - \lambda x_0^2 + \lambda L^2}{x_0 - \lambda x_0 + \lambda L} + wx \quad ,$$

538 (17)

539 where  $\lambda = K_1/K_2$ . For the geological model ( $G_1$ ) with homogenous hydraulic conductivity, i.e.,  
 540  $K = K_1 = K_2$ , Eq. (22) becomes

$$541 \quad q(x) = K \frac{h_1^2 - h_2^2}{2L} - \frac{1}{2} wL + wx \quad ,$$

542 (18)

543 which is the well-known solution available in hydrogeology textbooks. Using the analytical  
 544 solutions of  $q(x)$ , the MMADS method is implemented using Monte Carlo simulations based on  
 545 the pseudo code shown in Fig. 3.

#### 546 **4.2.2. Sensitivity Results for Individual System Models**

547 Table 3 lists the  $E_K(d\Delta)$  and  $V_K(d\Delta)$  values evaluated for the recharge, geology, and  
 548 snowmelt processes of the eight individual system models with consideration of parametric  
 549 uncertainty. If a process model has more than one parameter (e.g.,  $K_1$  and  $K_2$  associated with  
 550 process model  $G_2$ , and  $f_2$  and  $r$  associated with process model  $M_2$ ), the indices are evaluated for  
 551 the grouped parameters. Specifically speaking, the  $\theta_K$  term in Eqs. (4) and (5) includes two

552 parameters. For each system model, since  $E_K(d\Delta)$  and  $V_K(d\Delta)$  are evaluated for all parameters of  
553 each process,  $E_K(d\Delta)$  and  $V_K(d\Delta)$  measure influence of individual processes. Taking system  
554 model  $R_2G_2M_2$  as an example, the mean and variance of parameter  $b$  measure influence of the  
555 recharge process, those of parameters  $K_1$  and  $K_2$  measure influence of the geology process, and  
556 those of parameters  $f_2$  and  $r$  measure influence of the snowmelt process. Table 3 also lists the  
557 total-effect parameter sensitivity  $S_{Ti}$  (%) calculated by using SALib of Herman and Usher (2017).  
558  $S_{Ti}$  is used to quantitatively rank the three processes in terms of their influence within each  
559 system model, and the  $S_{Ti}$ -based process rank is used as a reference to evaluate MMADS results.

560 Table 3 shows that, for each system model, the process rank of MMADS is the same as that  
561 given by  $S_{Ti}$ , indicating that the MMADS results are reliable. The process rank changes  
562 substantially between system models, and any of the three processes can be ranked as the most  
563 influential (or the least influential) process. For example, in system model  $R_1G_1M_1$ , the recharge  
564 process is identified as the least influential process and the snowmelt process as the most  
565 influential process, whereas it is the opposite case for system model  $R_2G_2M_2$ . This is also  
566 observed in Fig. 4(b) that plots the three processes in three colors (recharge in red, geology in  
567 green, and snowmelt in blue). The open symbols of the eight individual system models are  
568 mixed, and do not reveal a pattern to indicate process influence under process model uncertainty.  
569 It is therefore necessary to use MMADS method for identifying non-influential processes for all  
570 the system models to address process model uncertainty.

571 For the individual system models, the MMADS results can reflect process interactions. This  
572 is made clear by examining the  $E_K(d\Delta)$  and  $V_K(d\Delta)$  values of  $R_1G_1M_1$  and  $R_2G_1M_1$ , which have  
573 different recharge models but the same geology and snowmelt models. For the two system

574 models with homogeneous hydraulic conductivity, based on Eq. (18), the groundwater discharge  
 575 per unit width at  $x_0 = 7,000$  m (which equals to  $0.7L$ ) is

$$576 \quad q(x_0) = K \frac{h_1^2 - h_2^2}{2L} + 0.2wL. \quad (19)$$

577 This equation shows that  $w$  does not interact with  $K$  or  $h_2$ , indicating that the recharge process  
 578 does not interact with the geology or snowmelt process. As a results, between  $R_1G_1M_1$  and  
 579  $R_2G_1M_1$ , the  $E_K(d\Delta)$  and  $V_K(d\Delta)$  values of  $a$  (the recharge model parameter) change, but those of  
 580  $K$  (the geology model parameter) and  $f_1$  (the snowmelt model parameter) do not change. This is  
 581 not surprising in the context of MMADS calculation. To evaluate the output difference ( $d\Delta$ )  
 582 caused by the variation of parameter  $K$  of the geology process, parameter  $a$  or  $b$  of the recharge  
 583 process (Eq. (12)) and parameter  $f_1$  of the snowmelt process (Eq. (16)) are fixed. Since the  
 584 recharge and geology processes do not interact, the second term,  $0.2wL$ , in Eq. (19) does not  
 585 affect  $d\Delta$  due to change of  $K$ , which means that  $d\Delta$  is not affected by parameter  $a$  or  $b$ .  
 586 Therefore, the  $d\Delta$  value for  $K$  is the same for  $R_1G_1M_1$  and  $R_2G_1M_1$ . On the other hand, the  
 587 process interaction is reflected in the  $E_K(d\Delta)$  and  $V_K(d\Delta)$  values of  $R_1G_1M_1$  and  $R_1G_1M_2$ . These  
 588 values of  $K$  and  $f_1$  for  $R_1G_1M_1$  are different from those of  $K$  and  $f_2 \& r$  for  $R_1G_1M_2$  because the  
 589 interaction between  $K$  and  $f_1$  is different from the interaction between  $K$  and  $f_2 \& r$ , as indicated by  
 590 Eq. (19).

### 591 **4.2.3. Sensitivity Results for Multiple System Models**

592 In this numerical experiment,  $E_K(d\Delta)$  and  $V_K(d\Delta)$  are evaluated numerically using Monte  
 593 Carlo simulations based on the procedure discussed in Section 3.2. The cumulative distribution  
 594 of each parameter is divide into  $n = 5,000$  equal strata to generate 5,000 LHS parameter samples.  
 595 Fig. 6 illustrates convergence of  $E_K(d\Delta)$  and  $V_K(d\Delta)$  of the three processes for the multiple

596 system models (convergence for individual system models not shown here). The 95% confidence  
597 intervals shown in Fig. 6 are estimated by using 100 bootstrapping resamples to assess the effect  
598 of sampling uncertainty and to evaluate robustness of the estimator to sample variability (Archer,  
599 et al., 1997; Yang et al., 2011). Fig. 6 shows that the  $E_K(d\Delta)$  and  $V_K(d\Delta)$  values converge after  
600 about 350 parameter realizations, and the corresponding total number of model executions is  
601  $980,000 = 2 \times 2 \times 350 \times 2 \times 350$ . A discussion on computational cost of MMADS is given in  
602 Section 5.

603 Table 3 lists the  $E_K(d\Delta)$  and  $V_K(d\Delta)$  values of the recharge, geology, and snowmelt processes  
604 with consideration of both process model and parametric uncertainty. The two sensitivity  
605 measures listed in Table 3 are estimated by using all 5,000 parameter realizations, and the  
606 corresponding number of model executions is  $200,000,000 = 2 \times 2 \times 5000 \times 2 \times 5000$ . The large  
607 number of model executions is affordable in this numerical example due to the use of analytical  
608 solutions of  $q_0$ , and the numerical results shown in Table 3 are accurate enough for identifying  
609 non-influential processes. A discussion on computational cost of MMADS is given in Section 5.  
610 MMADS identifies the snowmelt process as the most influential one, followed by the geology  
611 process, and then the recharge process. This is also observed in Fig. 4(b) that plots  $E_K(d\Delta)$  and  
612  $\sqrt{V_K(d\Delta)}$  for the three processes using cross symbols in three colors. The snowmelt process has  
613 the largest  $E_K(d\Delta)$  and  $V_K(d\Delta)$  values, substantially larger than those of the geology and recharge  
614 process. This may be due to the nonlinear effect of the snowmelt process (reflected by the  $h_2^2$   
615 term in Eqs. (17) or (18)) and the interaction between the snowmelt and geology processes  
616 discussed above. Due to the qualitative nature of MMADS, using it to explain the nonlinear  
617 effect and process interactions is not straightforward.

618

## 619 **5. Further Investigation and Discussion**

### 620 **5.1 Computational Cost and Robustness of MMADS**

621 Although  $200,000,000 = 2 \times 2 \times 5,000 \times 2 \times 5,000$  model executions are used for the  
622 groundwater example, the high computational cost is unnecessarily and can be substantially  
623 reduced in practice. To determine the smallest number of model executions that can give  
624 accurate results for the groundwater flow modeling example, we gradually increase the number,  
625  $n$ , of parameter realizations from 10 to 400, and evaluate a criterion called robustness by  
626 following Razavi and Gupta (2016) and Sheikholeslami et al. (2019). For each  $n$  value,  $E_K(d\Delta)$   
627 and  $V_K(d\Delta)$  of the three processes are estimated by 100 numerical experiments with 100  
628 different sets of random parameter samples. Based on the  $E_K(d\Delta)$  and  $V_K(d\Delta)$  values, we count  
629 how many times when snowmelt is identified by MMADS as the most influential process,  
630 geology as the second most influential process, and recharge as the least influential process (the  
631 process ranking is obtained above using 200 million model executions). Dividing the numbers by  
632 100 gives MMADS robustness (%) for identifying influential processes. The results are plotted  
633 in Fig. 7 for the three processes. The figure shows that MMADS is almost 100% robust to  
634 identify snowmelt as the most influential process, even for a small number ( $n$ ) of parameter  
635 realizations. When  $n$  is small, MMADS cannot corrected identify recharge as the least influential  
636 process or identify geology as the second least influential process. The MMADS robustness is  
637 the same for ranking the recharge and geology processes, because the groundwater example  
638 considers only three processes and snowmelt is always identified as the most influential process.  
639 An important observation from Fig. 7 is that the MMADS results are accurate enough (with  
640 robustness larger than 95%) when using  $n = 20$  parameter realizations. The corresponding  
641 number of model executions is  $3,200 = 2 \times 2 \times 20 \times 2 \times 20$ , substantially smaller than the

642 number of 200 million model executions. This number of model executions is expected to be  
643 computationally affordable for moderate models with nowadays computational resources  
644 available to general molders. In addition, the model executions are independent and can be  
645 conducted in parallel, which can further improve computational efficiency of MMADS.

646

## 647 **5.2 Effects of Process Model Probabilities on MMADS Method**

648 The numerical experiments above assume equal probabilities for alternative process models,  
649 whereas it is likely that the models have different probabilities. To explore the effects of process  
650 model probabilities on  $E_K(d\Delta)$  and  $V_K(d\Delta)$ , we evaluate the mean and variance for the  
651 groundwater flow modeling example using different sets of process model probabilities. For the  
652 groundwater experiment, since each process has two alternative models and the sum of their  
653 probabilities is one (e.g.,  $P(R_1) + P(R_2) = 1.0$  for the recharge process), we only need to vary  
654 probabilities of three process models, one for each process. We thus vary  $P(R_1)$ ,  $P(G_1)$ , and  
655  $P(M_1)$ , and generate their values from the standard uniform distribution  $U[0,1]$ . Therefore, for  
656 each process, a random number  $r$  is sampled for from the uniform distribution,  $U[0, 1]$ , and  
657 transformed into process probability values following the approach described by Moeini et al.  
658 (2011). Subsequently, Sobol's variance-based sensitivity analysis is conducted to determine  
659 sensitivity of  $E_K(d\Delta)$  and  $V_K(d\Delta)$  to process model probabilities, which is referred to as a  
660 sensitivity analysis of a sensitivity analysis (Paleari and Confalonieri, 2016; Puy et al., 2020).  
661 For estimating Sobol's first-order ( $S_i$ ) and total-effect ( $S_{Ti}$ ) sensitivity indices, we use the  
662 sampling scheme discussed in Saltelli et al. (2010) to generate two sampling matrices  $A$  and  $B$ .  
663 Each has the dimension of 1,000 rows  $\times$  3 columns, corresponding to 1,000 realizations of the  
664 model probabilities of  $P(R_1)$ ,  $P(G_1)$ , and  $P(M_1)$ . Based on  $A$  and  $B$ , three additional matrices are

665 generated, and each is denoted as  $C_i$  ( $i = 1, 2,$  and  $3$ ).  $C_i$  is a copy of  $A$ , but its column  $i$  is  
666 replaced with column  $i$  of matrix  $B$ .  $S_i$  and  $S_{Ti}$  are estimated using the 5,000 parameter sets of the  
667 five matrices. Estimating  $S_i$  and  $S_{Ti}$  does not require new  $d\Delta$  values, because the sensitivity  
668 analysis only changes process model probabilities.

669 Fig. 8 shows that the  $E(d\Delta)$  and  $V(d\Delta)$  values of the three processes change with model  
670 probabilities of the corresponding processes. For example, in Figs 8(a) and 8(d),  $E(d\Delta)$  and  
671  $V(d\Delta)$  of the recharge process vary with probability  $P(R_1)$  of model  $R_1$ . For all the three  
672 processes, their  $E_K(d\Delta)$  and  $V_K(d\Delta)$  values change when process model probability changes. The  
673 magnitude of changes is the largest for the snowmelt process (Figs. 8(c) and 8(f)). The variation  
674 patterns are different for the three processes. In Figs. 8(a) and 8(d) for the recharge process,  
675  $E_K(d\Delta)$  and  $V_K(d\Delta)$  generally decrease when  $P(R_1)$  increases. The variation pattern is the  
676 opposite for the geology process, as shown in Figs 8(b) and 8(e). For the snowmelt process, Figs.  
677 8(c) and 8(f) shows that  $E_K(d\Delta)$  and  $V_K(d\Delta)$  first increase and then decrease with the increase of  
678  $P(M_1)$ . The non-monotonic variation pattern indicates that using appropriate model probability  
679 values is important for MMADS to identifying non-influential processes. It should be noted that,  
680 although each plot of Fig. 8 only shows  $E_K(d\Delta)$  or  $V_K(d\Delta)$  changes with probability of one  
681 process model,  $E_K(d\Delta)$  and  $V_K(d\Delta)$  are also affected by probability of the other two process  
682 models. It is possible that inappropriate probability of one process model may affect  
683 identification influence of non-influence of another process. Investigating this is warranted in a  
684 future study.

685 We further examine to what extent process model probability affects identification of non-  
686 influential processes. For the 5,000 realizations of  $E_K(d\Delta)$  and  $V_K(d\Delta)$  values, we count how  
687 many times each process is identified as the most non-influential process (i.e., the process'

688  $E_K(d\Delta)$  and  $V_K(d\Delta)$  values are smaller than those of the other two processes). The recharge  
 689 process is identified as the most non-influential one for 2,758 out of 5,000 times (55.16%), the  
 690 geology process for 2,080 times (41.60%), the snowmelt process for 25 times (0.50%). These  
 691 quantitative results indicate again that using appropriate model probability values is important  
 692 for MMADS to identifying non-influential processes.

693 Fig. 9 illustrates Sobol's total-effect sensitivity index ( $S_{Ti}$ ) evaluated for  $E_K(d\Delta)$  and  $V_K(d\Delta)$   
 694 (the results of first-order sensitivity index ( $S_i$ ) are similar and thus not shown). The  $S_{Ti}$  values are  
 695 estimated for each process, and measure sensitivity of the process to  $P(R_1)$ ,  $P(G_1)$ , and  $P(M_1)$ .  
 696 Fig. 9(a) indicates that  $E_K(d\Delta)$  of the recharge process is most sensitive to  $P(R_1)$  and then to  
 697  $P(G_1)$  but not to  $P(M_1)$ . This is different for the geology and snowmelt processes, whose  $E_K(d\Delta)$   
 698 values are most sensitive to  $P(M_1)$ . This is especially the case for the snowmelt process. Fig. 9(b)  
 699 shows to what extent  $V_K(d\Delta)$  of each process is sensitive to  $P(R_1)$ ,  $P(G_1)$ , and  $P(M_1)$ . We observe  
 700 from Fig. 9 that  $E_K(d\Delta)$  and  $V_K(d\Delta)$  of a process are substantially sensitive to the process's model  
 701 probability, which is not surprising. While the sensitivity of one process'  $E_K(d\Delta)$  and  $V_K(d\Delta)$  to  
 702 other processes' model probability may be negligible, it is not always the case. This indicates  
 703 again that it is important to accurately estimate model probability of all processes for identifying  
 704 non-influential processes.

705

### 706 **5.3 Limitations and Future Work**

707 The MMADS method discussed in this study is subject to three limitations. The first  
 708 limitation is that the computational cost for  $(N_{M-k} \times n) \times (N_{M-k} \times n)$  number of model executions  
 709 may be high, especially for a large number ( $n$ ) of parameter realizations. Although Fig. 7  
 710 indicates that  $n = 20$  gives satisfactory results for the groundwater example, each process model

711 has only one or two parameters. When the number of random model parameters increase, the  
712 number of parameter realizations is expected to increase, and the curse of dimensionality may  
713 occur (Sheikholeslami et al., 2019). One way to reduce the computational cost of MMADS is to  
714 break the two nested loops of parameter realizations shown in Fig. 3, and this can be done by  
715 using the binning method that was used in Dai et al. (2017a, 2017b). The binning method  
716 reduces the number of model executions from the order of  $n^2$  to the order of  $n$ , and its  
717 implementation is straightforward. However, the binning method is not mathematically rigorous,  
718 and more theoretical development is needed in a future study.

719 The second limitation is that the derivation of  $E_K(d\Delta)$  and  $V_K(d\Delta)$  in Eqs. (4) and (5)  
720 implicitly assumes that the probabilities of process models and model parameters are  
721 independent. This assumption for parameters may be invalid in practice, and joint parameter  
722 distributions of a variety of forms may be needed (Lamboni and Kucherenko, 2021). After the  
723 joint distributions are determined, correlated parameter realizations can be generated using  
724 various approaches (e.g., LHS) for estimating  $E_K(d\Delta)$  and  $V_K(d\Delta)$  (Sallaberry et al., 2008; Xu  
725 and Gertner, 2008). For correlated process models, their joint probability has not been adequately  
726 studied. The Bayesian network of Dai et al. (2019) may potentially address the issue of process  
727 model correlation, but more in-depth investigation is needed.

728 The last limitation is the qualitative nature of the MMADS method. In the current study, a  
729 process is identified to be non-influential, if its  $E_K(d\Delta)$  and  $V_K(d\Delta)$  values are smaller than those  
730 of other processes. The identification is in a relatively sense, and it is possible for MMADS to  
731 identify the most influential or non-influential process. However, MMADS cannot quantify the  
732 extent that one process is more influential or non-influential than another process. On the other  
733 hand, if one is not interested in the most non-influential process but a set of processes that are

734 non-influential, MMADS does not provide a quantitative threshold to decisively identify the  
735 processes. While this problem may be addressed by using a clustering method discussed in  
736 Sheikholeslami et al. (2019), the drawback of MMADS is inherent in screening methods  
737 including the Morris screening method.

738

## 739 **6. Conclusions**

740 This study develops a new multi-model absolute difference-based sensitivity (MMADS)  
741 analysis method to identify non-influential system processes with consideration of uncertainty in  
742 both process model structures and process model parameters. MMADS is an extension of the  
743 Morris method from the parameter space to the parameter-model space, in which a system  
744 process may be represented by multiple process models. The absolute differences of a model  
745 output are first evaluated by considering not only process model variation but also process model  
746 parameter variation. The variations are quantified by the mean and variance of the differences,  
747 which are evaluated by using the model averaging approaches based on probabilities of process  
748 models. A process with small mean and variance is considered to be non-influential. To our  
749 knowledge, there does not exist a method like MMADS that explicitly considers uncertainty in  
750 process model structures and process model parameters and integrates the expended Morris  
751 method with model averaging methods.

752 The two numerical experiments employed in this study demonstrate the following: (1) the  
753 process ranking changes between alternative system models, which manifests the needs of  
754 identifying non-influential system processes under process model uncertainty and process model  
755 parametric uncertainty; (2) considering only parametric uncertainty may lead to biased  
756 identification of non-influential processes; (3) for the first numerical experiment with the Sobol's

757 G\*-function, the analytical solutions for the mean and variance of the multi-model differences  
758 verify the pseudo code and numerical code used to evaluate the mean and variance of MMADS;  
759 (3) the second numerical experiment of groundwater modeling with three interacting processes  
760 shows that the mean and variance of MMADS reflect interactions between geology and  
761 snowmelt processes and no interactions between the two processes and the recharge process.

762 The MMADS method, similar to the Morris method, plots the mean and standard deviation  
763 of the multi-model differences in a 2-D plane, and the plot can be used to visually identify non-  
764 influential system processes. For the numerical example of groundwater flow modeling,  
765 MMADS method can give a meaningful process ranking with a small number of model  
766 executions. In MMADS, the process model probabilities can play an important role in  
767 determining non-influential processes. Similar to the Morris method, MMADS method may be  
768 used as a screening tool for qualitatively identifying non-influential processes. While MMADS is  
769 used for differential-equation-based groundwater models in this study, the method can be applied  
770 to data-driven models that are developed using statistical and/or machine learning techniques,  
771 because applications of MMADS do not rely on knowing model structures but only need to  
772 consider transitions between models and model inputs. A further investigation on this is  
773 warranted.

#### 774 **Acknowledgments**

775 This research was supported in part by U.S. Department of Energy grant DE-SC0019438 and  
776 National Science Foundation grant EAR-1552329. Python codes and data used in this study are  
777 available at GitHub via <https://github.com/jyangfsu/MMADS>. We thank Associate Editor Saket  
778 Pande, reviewer Razi Sheikholeslami, and the other two anonymous reviewers for their insightful  
779 comments and suggestions, which greatly helped improve this manuscript.

780

781 **Appendix A: Derivation of  $E(d\Delta)$  and  $V(d\Delta)$  to include parametric uncertainty**

782 Eqs. (2) and (3) can be extended to include parametric uncertainty. Applying the law of total  
 783 expectation to the two expectations  $E_{\mathbf{M}_{-K}}$  and  $E_{T_{M_K}}$  in Eq. (2) leads to

$$784 \quad E_K(d\Delta) = E_{\mathbf{M}_{-K}} E_{T_{M_K}}(d\Delta | M_{-K}) = E_{\mathbf{M}_{-K}} E_{\theta_{-K}|M_{-K}} E_{T_{M_K}} E_{T_{\theta_K}|T_{M_K}}(d\Delta | \theta_{-K}, M_{-K}, T_{\theta_K}, T_{M_K}). \quad (\text{A1})$$

785 For the variance of  $d\Delta$  in Eq. (3), by first applying the law of the total expectation to  $E_{\mathbf{M}_{-K}}$  and

786  $E_{T_{M_K}}$ , we have

$$787 \quad V_K(d\Delta) = E_{\mathbf{M}_{-K}} E_{\theta_{-K}|M_{-K}} V_{T_{M_K}}(d\Delta | \theta_{-K}, M_{-K}) + V_{\mathbf{M}_{-K}} E_{T_{M_K}} E_{T_{\theta_K}|T_{M_K}}(d\Delta | M_{-K}, T_{\theta_K}, T_{M_K}). \quad (\text{A2})$$

788 According to the definition of the variance, the first term at the right-hand side of Eq. (A2) can  
 789 be rewritten as

$$\begin{aligned} & E_{\mathbf{M}_{-K}} E_{\theta_{-K}|M_{-K}} V_{T_{M_K}}(d\Delta | \theta_{-K}, M_{-K}) \\ 790 \quad &= E_{\mathbf{M}_{-K}} E_{\theta_{-K}|M_{-K}} \left( E_{T_{M_K}}(d\Delta | \theta_{-K}, M_{-K})^2 - \left( E_{T_{M_K}}(d\Delta | \theta_{-K}, M_{-K}) \right)^2 \right) \\ &= E_{\mathbf{M}_{-K}} E_{\theta_{-K}|M_{-K}} E_{T_{M_K}}(d\Delta | \theta_{-K}, M_{-K})^2 - E_{\mathbf{M}_{-K}} E_{\theta_{-K}|M_{-K}} \left( E_{T_{M_K}}(d\Delta | \theta_{-K}, M_{-K}) \right)^2 \end{aligned}$$

791 (A3)

792 Subsequently, applying the law of total expectation to  $E_{T_{M_K}}$ , Eq. (A3) becomes

$$\begin{aligned} & E_{\mathbf{M}_{-K}} E_{\theta_{-K}|M_{-K}} V_{T_{M_K}}(d\Delta | \theta_{-K}, M_{-K}) \\ 793 \quad &= E_{\mathbf{M}_{-K}} E_{\theta_{-K}|M_{-K}} E_{T_{M_K}} E_{T_{\theta_K}|T_{M_K}}(d\Delta | \theta_{-K}, M_{-K}, T_{\theta_K}, T_{M_K})^2 \\ &\quad - E_{\mathbf{M}_{-K}} E_{\theta_{-K}|M_{-K}} \left( E_{T_{M_K}} E_{T_{\theta_K}|T_{M_K}}(d\Delta | \theta_{-K}, M_{-K}, T_{\theta_K}, T_{M_K}) \right)^2 \end{aligned}$$

794 (A4)

795 Similarly, the second term at the right-hand side of Eq. (A2) can be rewritten as

$$\begin{aligned}
& V_{\mathbf{M}_{-K}} E_{T_{M_K}} E_{T_{\theta_K} | T_{M_K}} (d\Delta | M_{-K}, T_{\theta_K}, T_{M_K}) \\
&= E_{\mathbf{M}_{-K}} \left( E_{T_{M_K}} E_{T_{\theta_K} | T_{M_K}} (d\Delta | M_{-K}, T_{\theta_K}, T_{M_K}) \right)^2 - \left( E_{\mathbf{M}_{-K}} E_{T_{M_K}} E_{T_{\theta_K} | T_{M_K}} (d\Delta | M_{-K}, T_{\theta_K}, T_{M_K}) \right)^2 \\
796 &= E_{\mathbf{M}_{-K}} E_{\theta_{-K} | M_{-K}} \left( E_{T_{M_K}} E_{T_{\theta_K} | T_{M_K}} (d\Delta | \theta_{-K}, M_{-K}, T_{\theta_K}, T_{M_K}) \right)^2 \\
&\quad - \left( E_{\mathbf{M}_{-K}} E_{\theta_{-K} | M_{-K}} E_{T_{M_K}} E_{T_{\theta_K} | T_{M_K}} (d\Delta | \theta_{-K}, M_{-K}, T_{\theta_K}, T_{M_K}) \right)^2 \\
797 & \text{(A5)}
\end{aligned}$$

798 Substituting Eqs. (A4) and (A5) into Eq. (A2) leads to

$$\begin{aligned}
799 & V_K (d\Delta | K) = E_{\mathbf{M}_{-K}} E_{\theta_{-K} | M_{-K}} E_{T_{M_K}} E_{T_{\theta_K} | T_{M_K}} (d\Delta | \theta_{-K}, M_{-K}, T_{\theta_K}, T_{M_K})^2 \\
&\quad - \left( E_{\mathbf{M}_{-K}} E_{\theta_{-K} | M_{-K}} E_{T_{M_K}} E_{T_{\theta_K} | T_{M_K}} (d\Delta | \theta_{-K}, M_{-K}, T_{\theta_K}, T_{M_K}) \right)^2 \\
800 & \text{(A6)}
\end{aligned}$$

801

802

803

804

805

806

807

808

809 **Appendix B: Derivation of analytical solutions of  $E(d\Delta)$  and  $V(d\Delta)$  for a single system**

810 **model of Sobol's  $G^*$ -function**

811 The derivation is for system model  $\prod_{i=1}^{10} g_i^{*1}$  as an example. Without consideration of process  
 812 model uncertainty and according to Eq. (6), the mean of  $d\Delta$  caused by variation of parameter  
 813  $\theta_{g_1^{*1}}$  of process model  $g_1^{*1}$  is

$$\begin{aligned}
 E_K(d\Delta) &= E_{\theta_{g_1^{*1}}} E_{T_{\theta_{g_1^{*1}}}} (d\Delta | \theta_{g_1^{*1}}, T_{\theta_{g_1^{*1}}}) \\
 &= E_{\theta_{g_2^{*1}}, \dots, \theta_{g_{10}^{*1}}} E_{\theta_{g_1^{*1}} \rightarrow \theta'_{g_1^{*1}}} \left| \Delta | \theta_{g_2^{*1}}, \dots, \theta_{g_{10}^{*1}}, \theta'_{g_1^{*1}} - \Delta | \theta_{g_2^{*1}}, \dots, \theta_{g_{10}^{*1}}, \theta_{g_1^{*1}} \right|
 \end{aligned}$$

815 (B1)

816 Under the assumption of independent parameters and applying the law of total expectation, Eq.  
 817 (B1) can be re-arranged as

$$E_K(d\Delta) = E_{\theta_{g_2^{*1}}} \dots E_{\theta_{g_{10}^{*1}}} E_{\theta_{g_1^{*1}}} E_{\theta'_{g_1^{*1}}} \left| \Delta | \theta_{g_2^{*1}}, \dots, \theta_{g_{10}^{*1}}, \theta'_{g_1^{*1}} - \Delta | \theta_{g_2^{*1}}, \dots, \theta_{g_{10}^{*1}}, \theta_{g_1^{*1}} \right|$$

819 (B2)

820 Recalling that  $\Delta = \prod_{i=1}^{10} g_i^{*1}$ , Eq. (A2) can be rewritten as

$$\begin{aligned}
 E_K(d\Delta) &= E_{\theta_{g_2^{*1}}} \dots E_{\theta_{g_{10}^{*1}}} E_{\theta_{g_1^{*1}}} E_{\theta'_{g_1^{*1}}} \left| g_2^{*1}(\theta_{g_2^{*1}}) \dots g_{10}^{*1}(\theta_{g_{10}^{*1}}) g_1^{*1}(\theta'_{g_1^{*1}}) - g_2^{*1}(\theta_{g_2^{*1}}) \dots g_{10}^{*1}(\theta_{g_{10}^{*1}}) g_1^{*1}(\theta_{g_1^{*1}}) \right| \\
 &= E_{\theta_{g_2^{*1}}} \dots E_{\theta_{g_{10}^{*1}}} E_{\theta_{g_1^{*1}}} E_{\theta'_{g_1^{*1}}} g_2^{*1}(\theta_{g_2^{*1}}) \dots g_{10}^{*1}(\theta_{g_{10}^{*1}}) \left| g_1^{*1}(\theta'_{g_1^{*1}}) - g_1^{*1}(\theta_{g_1^{*1}}) \right| \\
 &= E_{\theta_{g_2^{*1}}} g_2^{*1}(\theta_{g_2^{*1}}) \dots E_{\theta_{g_{10}^{*1}}} g_{10}^{*1}(\theta_{g_{10}^{*1}}) E_{\theta_{g_1^{*1}}} E_{\theta'_{g_1^{*1}}} \left| g_1^{*1}(\theta'_{g_1^{*1}}) - g_1^{*1}(\theta_{g_1^{*1}}) \right|
 \end{aligned}$$

822 (B3)

823 Since the mean of each product element in the Sobol's G\*-function is one, Eq. (B3) can be  
 824 simplified to

825  $E_K(d\Delta) = E_{\theta_{g_1^{*1}}} E_{\theta'_{g_1^{*1}}} \left| g_1^{*1}(\theta'_{g_1^{*1}}) - g_1^{*1}(\theta_{g_1^{*1}}) \right|$

826 (B4)

827 Rewriting the expectations in Eq. (B4) as integrals leads to

828  $E_K(d\Delta) = \iint \left| g_1^{*1}(\theta'_{g_1^{*1}}) - g_1^{*1}(\theta_{g_1^{*1}}) \right| p_{\theta'_{g_1^{*1}}} p_{\theta_{g_1^{*1}}} d\theta'_{g_1^{*1}} d\theta_{g_1^{*1}}$

829 (B5)

830 where  $p_{\theta'_{g_1^{*1}}}$  and  $p_{\theta_{g_1^{*1}}}$  are the probability density functions of  $\theta'_{g_1^{*1}}$  and  $\theta_{g_1^{*1}}$ , respectively.

831 Recalling that each parameter ( $X_i$ ) of the Sobol's G\*-function follows uniform distribution U[0,1],

832 substituting the expression of  $g_1^{*1}$  based on Eq. (11) to Eq. (B5) leads to

833 
$$E_K(d\Delta) = \int_0^1 \int_0^1 \left| \frac{(1+\alpha_1^1) \cdot |2X_1 - 1|^{\alpha_1^1} + a_1^1}{1+a_1^1} - \frac{(1+\alpha_1^1) \cdot |2X_1 - 1|^{\alpha_1^1} + a_1^1}{1+a_1^1} \right| dX_1 dX_1$$

834 (B6)

835 The analytical solution of Eq. (B6) is

836 
$$E_K(d\Delta) = \frac{2\alpha_1^1}{(a_1^1 + 1)(\alpha_1^1 + 2)}$$

837 (B7)

838 For system model  $\prod_{i=1}^{10} g_i^{*1}$ , given that  $a_1^1 = 0.002$  and  $\alpha_1^1 = 1$  for  $g_1^{*1}$ , we have

839 
$$E_K(d\Delta) = \frac{2 \times 1}{(0.002 + 1) \times (1 + 2)} = \frac{2}{3.006} \approx 0.6653 \text{ for } g_1^{*1}.$$

840 To evaluate  $V(d\Delta)$  for  $g_1^{*1}$ , according to Eq. (7), we have

$$841 \quad V_K(d\Delta | g_1^{*1}) = E_{\theta_{g_1^{*1}}} E_{T_{\theta_{g_1^{*1}}}} (d\Delta | \theta_{g_1^{*1}}, T_{\theta_{g_1^{*1}}})^2 - \left( E_{\theta_{g_1^{*1}}} E_{T_{\theta_{g_1^{*1}}}} (d\Delta | \theta_{g_1^{*1}}, T_{\theta_{g_1^{*1}}}) \right)^2$$

842 (B8)

843 The second term at the right-hand side of Eq. (B8) equals  $(E_K(d\Delta))^2$ . Similar to the derivation

844 of Eqs. (B2) and (B3), the first term at the right-hand side of Eq. (B8) becomes

$$845 \quad \begin{aligned} & E_{\theta_{g_1^{*1}}} E_{T_{\theta_{g_1^{*1}}}} (d\Delta | \theta_{g_1^{*1}}, T_{\theta_{g_1^{*1}}})^2 \\ &= E_{\theta_{g_2^{*1}}} \left( g_2^{*1}(\theta_{g_2^{*1}}) \right)^2 \dots E_{\theta_{g_{10}^{*1}}} \left( g_{10}^{*1}(\theta_{g_{10}^{*1}}) \right)^2 E_{\theta_{g_1^{*1}}} E_{T_{\theta_{g_1^{*1}}}} \left| g_1^{*1}(\theta_{g_1^{*1}}) - g_1^{*1}(\theta_{g_1^{*1}}) \right|^2 \end{aligned}$$

846 (B9)

847 Based on the definition of variance, we have

$$848 \quad E_{\theta_{g_2^{*1}}} \left( g_2^{*1}(\theta_{g_2^{*1}}) \right)^2 = \left( E_{\theta_{g_2^{*1}}} g_2^{*1}(\theta_{g_2^{*1}}) \right)^2 + V_{\theta_{g_2^{*1}}}$$

849 (B10)

850 Since the mean of each product element is 1 and the variance of each product element in the

851 Sobol's  $G^*$ -function is  $\frac{\alpha_i^{j^2}}{(1+2\alpha_i^j)(1+a_i^j)^2}$ , Eq. (B10) becomes

$$852 \quad E_{\theta_{g_2^{*1}}} \left( g_2^{*1}(\theta_{g_2^{*1}}) \right)^2 = 1 + V_2^1$$

853 (B11)

854 where  $V_2^1$  represents the variance of  $g_2^{*1}$  which can be calculate as  $\frac{(\alpha_2^1)^2}{(1+2\alpha_2^1)(1+a_2^1)^2}$ .

855 Accordingly,

$$856 \quad E_{\theta_{g_i^{*1}}} \left( g_i^{*1}(\theta_{g_i^{*1}}) \right)^2 = 1 + V_i^1$$

857 (B12)

858 where  $V_i^1$  represents the variance of  $g_i^{*1}$  which can be calculate as  $\frac{(\alpha_i^1)^2}{(1+2\alpha_i^1)(1+a_i^1)^2}$  .

859 Substituting Eq. (B12) to Eq. (A9) leads to

$$860 \quad E_{\theta_{g_1^{*1}}} E_{T_{\theta_{g_1^{*1}}}} (d\Delta | \theta_{g_1^{*1}}, T_{\theta_{g_1^{*1}}})^2$$

$$= (1+V_2^1) \dots (1+V_{10}^1) E_{\theta_{g_1^{*1}}} E_{T_{\theta_{g_1^{*1}}}} \left| g_1^{*1}(\theta'_{g_1^{*1}}) - g_1^{*1}(\theta_{g_1^{*1}}) \right|^2$$

861 (B13)

862 Rewriting the expectations in Eq. (B13) as integrals leads to

$$E_{\theta_{g_1^{*1}}} E_{T_{\theta_{g_1^{*1}}}} (d\Delta | \theta_{g_1^{*1}}, T_{\theta_{g_1^{*1}}})^2$$

$$= (1+V_2^1) \dots (1+V_{10}^1) \iint \left| g_1^{*1}(\theta'_{g_1^{*1}}) - g_1^{*1}(\theta_{g_1^{*1}}) \right|^2 p(\theta'_{g_1^{*1}}) p(\theta_{g_1^{*1}}) d\theta'_{g_1^{*1}} d\theta_{g_1^{*1}}$$

$$863 \quad = (1+V_2^1) \dots (1+V_{10}^1) \iint \left| g_1^{*1}(\theta'_{g_1^{*1}}) - g_1^{*1}(\theta_{g_1^{*1}}) \right|^2 d\theta'_{g_1^{*1}} d\theta_{g_1^{*1}}$$

$$= (1+V_2^1) \dots (1+V_{10}^1) \int_0^1 \int_0^1 \left| \frac{(1+\alpha_1^1) \cdot |2X_1 - 1|^{\alpha_1^1} + a_1^1}{1+a_1^1} - \frac{(1+\alpha_1^1) \cdot |2X_1 - 1|^{\alpha_1^1} + a_1^1}{1+a_1^1} \right|^2 dX_1 dX_1'$$

864 (B14)

865 The analytical solution of Eq. (B14) is

$$E_{\theta_{g_1^{*1}}} E_{T_{\theta_{g_1^{*1}}}} (d\Delta | \theta_{g_1^{*1}}, T_{\theta_{g_1^{*1}}})^2$$

$$866 \quad = (1+V_2^1) \dots (1+V_{10}^1) \frac{1}{(2\alpha_1^1 + 1)} \frac{2(\alpha_1^1)^2}{(a_1^1 + 1)^2}$$

867 (B15)

868 For system model  $\prod_{i=1}^{10} g_i^{*1}$  and the  $a$  and  $\alpha$  values given in Table 1, we have

$$869 \quad V_2^1 = \frac{1}{(1+2) \times (1+0.08)^2} = \frac{1}{3.4992} \quad , \dots \quad V_{10}^1 = \frac{1}{(1+2) \times (1+85)^2} = \frac{1}{22188} \quad , \quad \text{and}$$

870  $E_{\theta_{g_1^*}} E_{T_{\theta_{g_1^*}}} (d\Delta | \theta_{g_1^*}, T_{\theta_{g_1^*}})^2 = \left(1 + \frac{1}{3.4992}\right) \times \dots \times \left(1 + \frac{1}{22188}\right) \times \frac{1}{2+1} \times \frac{2}{(0.002+1)^2} \approx 0.9522$  . As a

871 result, we have  $V_K(d\Delta | g_1^*) \approx 0.9522 - 0.6653^2 = 0.5096$  . Based on the above derivation, the

872 analytical expressions for the mean and variance of  $d\Delta$  under single system model of the Sobol's

873 G\*-function can be easily obtained, and thus not given here.

874 **Appendix C: Derivation of analytical solutions of  $E(d\Delta)$  and  $V(d\Delta)$  for multiple system**  
875 **models of Sobol's  $G^*$ -function**

876 For the Sobol's  $G^*$ -function  $\prod_{i=1}^{10} g_i^*$  under multiple system models, according to Eq. (4) and

877 replacing  $K$  by  $g_1^*$  and  $\sim K$  by  $g_2^* \dots g_{10}^*$  the mean of output difference ( $d\Delta$ ) of process  $g_1^*$  is

$$\begin{aligned}
& E_K(d\Delta) \\
878 &= E_{M_{g_1^*}} E_{\theta_{g_1^*} | M_{g_1^*}} E_{T_{M_{g_1^*}}} E_{T_{\theta_{g_1^*} | T_{M_{g_1^*}}}} (d\Delta | \theta_{g_1^*}, M_{g_1^*}, T_{\theta_{g_1^*}}, T_{M_{g_1^*}}) \\
&= E_{M_{g_2^* \dots g_{10}^*}} E_{\theta_{g_2^* \dots g_{10}^*} | M_{g_2^* \dots g_{10}^*}} E_{T_{M_{g_2^* \dots g_{10}^*}}} E_{T_{\theta_{g_2^* \dots g_{10}^*} | T_{M_{g_2^* \dots g_{10}^*}}}} (d\Delta | \theta_{g_2^* \dots g_{10}^*}, M_{g_2^* \dots g_{10}^*}, T_{\theta_{g_2^* \dots g_{10}^*}}, T_{M_{g_2^* \dots g_{10}^*}})
\end{aligned}$$

879 (C1)

880 Under the assumption of independent parameters, Eq. (C1) becomes

$$\begin{aligned}
& E_K(d\Delta) \\
881 &= E_{M_{g_2^*}} \dots E_{M_{g_{10}^*}} E_{\theta_{g_2^*} | M_{g_2^*}} \dots E_{\theta_{g_{10}^*} | M_{g_{10}^*}} E_{T_{M_{g_2^*}}} E_{T_{\theta_{g_2^*} | T_{M_{g_2^*}}}} (d\Delta | \theta_{g_2^*}, M_{g_2^*}, \dots, \theta_{g_{10}^*}, M_{g_{10}^*}, T_{\theta_{g_2^*}}, T_{M_{g_2^*}})
\end{aligned}$$

882 (C2)

883 Since there are two process models ( $g_1^{*1}$  and  $g_1^{*2}$ ) for  $g_1^*$ , the set of process model transitions is

884  $T_{M_{g_1^*}} = \{M_{g_1^{*1}} \rightarrow M_{g_1^{*1}}, M_{g_1^{*1}} \rightarrow M_{g_1^{*2}}, M_{g_1^{*2}} \rightarrow M_{g_1^{*1}}, M_{g_1^{*2}} \rightarrow M_{g_1^{*2}}\}$  . Considering that

885  $P(M_{g_1^{*i}} \rightarrow M_{g_1^{*j}}) = P(M_{g_1^{*i}})P(M_{g_1^{*j}})$  ( $i, j = 1, 2$ ), Eq.(C2) can be expanded as

$$\begin{aligned}
& E_K(d\Delta) \\
886 &= \sum_{k=1}^2 \dots \sum_{l=1}^2 E_{\theta_{g_2^*}^{*k}} \dots E_{\theta_{g_{10}^*}^{*l}} \left( \sum_{i=1}^2 \sum_{j=1}^2 P(M_{g_1^{*i}}) P(M_{g_1^{*j}}) E_{\theta_{g_1^{*i}}} E_{\theta_{g_1^{*j}}} \left| \begin{array}{l} \Delta | \theta_{g_2^*}^{*k}, M_{g_2^*}^{*k}, \theta_{g_3^*}^{*l}, M_{g_3^*}^{*l}, \theta_{g_1^*}^{*i}, M_{g_1^*}^{*i} \\ -\Delta | \theta_{g_2^*}^{*k}, M_{g_2^*}^{*k}, \theta_{g_3^*}^{*l}, M_{g_3^*}^{*l}, \theta_{g_1^*}^{*j}, M_{g_1^*}^{*j} \end{array} \right. \right) P(M_{g_2^*}^{*k}) \dots P(M_{g_{10}^*}^{*l}) \right) \quad . \quad (C3)
\end{aligned}$$

887 Note that there are nine summation symbols  $\sum_{k=1}^2 \dots \sum_{l=1}^2$  for processes  $g_2^* \dots g_{10}^*$  at the right-hand side

888 of Eq. (C3). Recalling that  $\theta$  here is variable  $X_i$  that follow the uniform distribution,  $U[0,1]$ ,

889 explicitly writing the expectations with respect to parameters in Eq. (C3) as integrals gives

$$\begin{aligned}
& E_K(d\Delta) \\
890 \quad & = \sum_{k=1}^2 \dots \sum_{l=1}^2 \iint \left( \sum_{i=1}^2 \sum_{j=1}^2 P(M_{g_{1i}^{*i}}) P(M_{g_{1j}^{*j}}) \iint \left| \Delta \left| \theta_{g_2^{*k}}, M_{g_2^{*k}}, \theta_{g_3^{*l}}, M_{g_3^{*l}}, \theta_{g_1^{*i}}, M_{g_1^{*i}} \right. \right. \right. \\
& \quad \left. \left. \left. - \Delta \left| \theta_{g_2^{*k}}, M_{g_2^{*k}}, \theta_{g_3^{*l}}, M_{g_3^{*l}}, \theta_{g_1^{*j}}, M_{g_1^{*j}} \right. \right. \right. \left. \left. \left. \right| d_{\theta_{g_1^{*i}}} d_{\theta_{g_1^{*j}}} \right) d_{\theta_{g_2^{*k}}} \dots d_{\theta_{g_{10}^{*l}}} P(M_{g_2^{*k}}) \dots P(M_{g_{10}^{*l}}) \right). \quad (C4)
\end{aligned}$$

891 Considering that the system output  $\Delta$  is the products of the three processes ( $\Delta = \prod_{i=1}^{10} g_i^*$ ) and that

892 the process models are equally weighted at 0.5, Eq. (C4) becomes

$$\begin{aligned}
& E_K(d\Delta) \\
893 \quad & = \frac{1}{2^{11}} \sum_{k=1}^2 \dots \sum_{l=1}^2 \iint \left( \sum_{i=1}^2 \sum_{j=1}^2 \iint \left| g_2^{*k}(\theta_{g_2^{*k}}) \times g_3^{*l}(\theta_{g_3^{*l}}) \times g_1^{*i}(\theta_{g_1^{*i}}) \right. \right. \\
& \quad \left. \left. \left. - g_2^{*k}(\theta_{g_2^{*k}}) \times g_3^{*l}(\theta_{g_3^{*l}}) \times g_1^{*j}(\theta_{g_1^{*j}}) \right. \right. \left. \left. \right| d_{\theta_{g_1^{*i}}} d_{\theta_{g_1^{*j}}} \right) d_{\theta_{g_2^{*k}}} \dots d_{\theta_{g_{10}^{*l}}} \\
& = \frac{1}{2^{11}} \sum_{k=1}^2 \dots \sum_{l=1}^2 \iint \left( \sum_{i=1}^2 \sum_{j=1}^2 \iint \left| g_1^{*i}(\theta_{g_1^{*i}}) - g_1^{*j}(\theta_{g_1^{*j}}) \right| d_{\theta_{g_1^{*i}}} d_{\theta_{g_1^{*j}}} \right) g_2^{*k}(\theta_{g_2^{*k}}) \dots g_{10}^{*l}(\theta_{g_{10}^{*l}}) d_{\theta_{g_2^{*k}}} \dots d_{\theta_{g_{10}^{*l}}}
\end{aligned}$$

894 (C5)

895 where  $\frac{1}{2^{11}}$  denotes the multiplication of the eleven  $P(M)$  terms in Eq. (C4). Recalling that the

896 mean of each product element  $g_i^*$  in the Sobol-G\* function is one, Eq. (C5) is further simplified

897 as

$$898 \quad E_K(d\Delta) = \frac{1}{2^{11}} \times 2^9 \times \sum_{i=1}^2 \sum_{j=1}^2 \iint \left| g_1^{*i}(\theta_{g_1^{*i}}) - g_1^{*j}(\theta_{g_1^{*j}}) \right| d_{\theta_{g_1^{*i}}} d_{\theta_{g_1^{*j}}} .$$

899 (C6)

900 Similarly, the mean values of  $d\Delta$  for the other nine processes  $g_k^*$  is evaluated via

$$901 \quad E_K(d\Delta) = \frac{1}{2^{11}} \times 2^9 \times \sum_{i=1}^2 \sum_{j=1}^2 \iint \left| g_k^{*i}(\theta_{g_k^{*i}}) - g_k^{*j}(\theta_{g_k^{*j}}) \right| d_{\theta_{g_k^{*i}}} d_{\theta_{g_k^{*j}}} .$$

902 (C7)

903 While analytical expressions of Eq. (C7) can be obtained in the way of deriving Eqs. (B6) and

904 (B7), the expressions are complicated because four parameters ( $\alpha_1^1, \alpha_1^2, a_1^1$  and  $a_1^2$ ) are involved.

905 We thus use the *scipy.integrate* function *dblquad* in Python to evaluate the double integrals  
 906 numerically.

907 To evaluate the variance of  $d\Delta$  for process  $g^*_1$  based on Eq. (5), replacing  $K$  by  $g^*_1$  and  $\sim K$   
 908 by  $g^*_2 \dots g^*_{10}$  gives

$$909 \quad V_K(d\Delta) = E_{M^*_{-g_1}} E_{\theta^*_{-g_1} | M^*_{-g_1}} E_{T_{M^*_{g_1}}} E_{T_{\theta^*_{g_1} | T_{M^*_{g_1}}}} (d\Delta | \theta^*_{-g_1}, M^*_{-g_1}, T_{\theta^*_{g_1}}, T_{M^*_{g_1}})^2$$

$$- \left( E_{M^*_{g_2 \dots g_{10}}} E_{\theta^*_{g_2 \dots g_{10}} | M^*_{g_2 \dots g_{10}}} E_{T_{M^*_{g_1}}} E_{T_{\theta^*_{g_1} | T_{M^*_{g_1}}}} (d\Delta | \theta^*_{g_2 \dots g_{10}}, M^*_{g_2 \dots g_{10}}, T_{\theta^*_{g_1}}, T_{M^*_{g_1}}) \right)^2$$

910 (C8)

911 The second term at the right-hand side of Eq. (C8) equals  $(E(d\Delta))^2$ , which can be calculated  
 912 based on Eq. (B6). Similar to the derivation of Eq.s (B2) and (B3), the first term at the right-hand  
 913 side of Eq. (C8) can be rewritten as

$$914 \quad E_{M^*_{-g_1}} E_{\theta^*_{-g_1} | M^*_{-g_1}} E_{T_{M^*_{g_1}}} E_{T_{\theta^*_{g_1} | T_{M^*_{g_1}}}} (d\Delta | \theta^*_{-g_1}, M^*_{-g_1}, T_{\theta^*_{g_1}}, T_{M^*_{g_1}})^2$$

$$= \sum_{k=1}^2 \dots \sum_{l=1}^2 E_{\theta^*_{g_2}^{*k}} \dots E_{\theta^*_{g_{10}}^{*l}} \left( \sum_{i=1}^2 \sum_{j=1}^2 P(M^*_{g_1}^{*i}) P(M^*_{g_1}^{*j}) E_{\theta^*_{g_1}^{*i}} E_{\theta^*_{g_1}^{*j}} \left| \begin{array}{l} \Delta | \theta^*_{g_2}^{*k}, M^*_{g_2}^{*k}, \theta^*_{g_3}^{*l}, M^*_{g_3}^{*l}, \theta^*_{g_1}^{*i}, M^*_{g_1}^{*i} \\ -\Delta | \theta^*_{g_2}^{*k}, M^*_{g_2}^{*k}, \theta^*_{g_3}^{*l}, M^*_{g_3}^{*l}, \theta^*_{g_1}^{*j}, M^*_{g_1}^{*j} \end{array} \right|^2 \right) P(M^*_{g_2}^{*k}) \dots P(M^*_{g_{10}}^{*l}) \right) \quad .(C9)$$

915 Recalling that for the Sobol's G\*-function,  $\Delta = \prod_{i=1}^{10} g^*_i$  and based on the derivation of Eq.s (B9) ~

916 (B13), Eq. (C9) can be rewritten as

$$917 \quad E_{M^*_{-g_1}} E_{\theta^*_{-g_1} | M^*_{-g_1}} E_{T_{M^*_{g_1}}} E_{T_{\theta^*_{g_1} | T_{M^*_{g_1}}}} (d\Delta | \theta^*_{-g_1}, M^*_{-g_1}, T_{\theta^*_{g_1}}, T_{M^*_{g_1}})^2$$

$$= \sum_{k=1}^2 \dots \sum_{l=1}^2 (1 + V_2^k) \dots (1 + V_{10}^l) \left( \sum_{i=1}^2 \sum_{j=1}^2 P(M^*_{g_1}^{*i}) P(M^*_{g_1}^{*j}) E_{\theta^*_{g_1}^{*i}} E_{\theta^*_{g_1}^{*j}} \left| g_1^{*i}(\theta^*_{g_1}^{*i}) - g_1^{*j}(\theta^*_{g_1}^{*j}) \right|^2 \right) P(M^*_{g_2}^{*k}) \dots P(M^*_{g_{10}}^{*l})$$

918 (C10)

919 where  $V_2^k$ , ..., and  $V_{10}^l$  denote the variance of element  $g_2^{*k}$ , ..., and  $g_{10}^{*l}$ , respectively.

920 Considering that the process models are equally weighted and each parameter follows uniform  
 921 distribution U[0,1], rewriting the expectations in Eq. (C10) as integrals leads to

$$\begin{aligned}
& E_{\mathbf{M}_{g_1^*}} E_{\boldsymbol{\theta}_{g_1^*} | \mathbf{M}_{g_1^*}} E_{T_{M_{g_1^*}}} E_{T_{\boldsymbol{\theta}_{g_1^*}} | T_{M_{g_1^*}}} (d\Delta | \boldsymbol{\theta}_{g_1^*}, \mathbf{M}_{g_1^*}, T_{\boldsymbol{\theta}_{g_1^*}}, T_{M_{g_1^*}})^2 \\
922 \quad &= \frac{1}{2^9} \sum_{k=1}^2 \sum_{l=1}^2 (1+V_2^k) \dots (1+V_{10}^l) \left( \sum_{i=1}^2 \sum_{j=1}^2 \frac{1}{2^2} E_{\boldsymbol{\theta}_{g_1^{*i}}} E_{\boldsymbol{\theta}_{g_1^{*j}}} \left| g_1^{*i}(\boldsymbol{\theta}_{g_1^{*i}}) - g_1^{*j}(\boldsymbol{\theta}_{g_1^{*j}}) \right|^2 \right) \\
&= \frac{1}{2^{11}} \sum_{k=1}^2 \sum_{l=1}^2 (1+V_2^k) \dots (1+V_{10}^l) \left( \sum_{i=1}^2 \sum_{j=1}^2 \iint \left| g_1^{*i}(\boldsymbol{\theta}_{g_1^{*i}}) - g_1^{*j}(\boldsymbol{\theta}_{g_1^{*j}}) \right|^2 d_{\boldsymbol{\theta}_{g_1^{*i}}} d_{\boldsymbol{\theta}_{g_1^{*j}}} \right)
\end{aligned}$$

923 (C11)

924 Substitute Eqs. (C6) and (C11) to (C8) gives

$$\begin{aligned}
925 \quad V_K(d\Delta) &= \frac{1}{2^{11}} \sum_{k=1}^2 \dots \sum_{l=1}^2 (1+V_2^k) \dots (1+V_{10}^l) \left( \sum_{i=1}^2 \sum_{j=1}^2 \iint \left| g_1^{*i}(\boldsymbol{\theta}_{g_1^{*i}}) - g_1^{*j}(\boldsymbol{\theta}_{g_1^{*j}}) \right|^2 d_{\boldsymbol{\theta}_{g_1^{*i}}} d_{\boldsymbol{\theta}_{g_1^{*j}}} \right) \\
&\quad - \left( \frac{1}{2^{11}} \times 2^9 \times \sum_{i=1}^2 \sum_{j=1}^2 \iint \left| g_1^{*i}(\boldsymbol{\theta}_{g_1^{*i}}) - g_1^{*j}(\boldsymbol{\theta}_{g_1^{*j}}) \right| d_{\boldsymbol{\theta}_{g_1^{*i}}} d_{\boldsymbol{\theta}_{g_1^{*j}}} \right)^2
\end{aligned}$$

926 (C12)

927 Eqs. (C12) is also numerically evaluated using the *scipy.integrate* function *dblquad*. Similarly,

928 the variance of  $d\Delta$  for other nine processes could be obtained.

929 **References**

- 930 Archer, G. E. B., Saltelli, A., Sobol, I. M. (1997). Sensitivity measures, ANOVA-like techniques  
931 and the use of bootstrap. *Journal of Statistical Computation and Simulation*, 58 (2),  
932 99e120. <https://doi.org/10.1080/00949659708811825>
- 933 Baroni, G. and Tarantola, S. (2014) A General Probabilistic Framework for uncertainty and  
934 global sensitivity analysis of deterministic models: A hydrological case study.  
935 *Environmental Modelling & Software* 51, 26-34.  
936 <https://doi.org/10.1016/j.envsoft.2013.09.022>
- 937 Becker, W.E., Tarantola, S. and Deman, G. (2018). Sensitivity analysis approaches to high-  
938 dimensional screening problems at low sample size. *Journal of Statistical Computation*  
939 *and Simulation* 88(11), 2089-2110. <https://doi.org/10.1080/00949655.2018.1450876>
- 940 Beven, K. J. (2002). Chapter 12 Uncertainty and the detection of structural change in models of  
941 environmental systems. *Developments in Environmental Modelling*, 22, 227-250.  
942 [https://doi.org/10.1016/S0167-8892\(02\)80013-6](https://doi.org/10.1016/S0167-8892(02)80013-6)
- 943 Bredehoeft, J. D. (2003). From models to performance assessment: the conceptualization  
944 problem. *Ground Water*, 41(5), 571-577. [https://doi.org/10.1111/j.1745-](https://doi.org/10.1111/j.1745-6584.2003.tb02395.x)  
945 [6584.2003.tb02395.x](https://doi.org/10.1111/j.1745-6584.2003.tb02395.x)
- 946 Bredehoeft, J. (2005). The conceptualization model problem-surprise. *Hydrogeology Journal*, 13,  
947 37–46. <https://doi.org/10.1007/s10040-004-0430-5>
- 948 Brenner, S., Coxon, G., Howden, N.J.K., Freer, J., and Hartmann, A. (2018). Process-based  
949 modelling to evaluate simulated groundwater levels and frequencies in a Chalk catchment  
950 in south-western England. *Natural Hazards and Earth System Sciences*, 18(2), 445-461.

951 <https://doi.org/10.5194/nhess-18-445-2018>

952 Campolongo, F., Cariboni, J., and Saltelli, A. (2007). An effective screening design for  
953 sensitivity analysis of large models. *Environmental Modelling & Software*, 22(10), 1509-  
954 1518. <https://doi.org/10.1016/j.envsoft.2006.10.004>

955 Chitsazan, N. and Tsai F. (2014). A hierarchical Bayesian model averaging framework for  
956 groundwater prediction under uncertainty, *Groundwater*, 53(2), 305-316,  
957 <https://doi.org/10.1111/gwat.12207>

958 Ciric, C., Ciffroy, P., and Charles, S. (2012). Use of sensitivity analysis to identify influential and  
959 non-influential parameters within an aquatic ecosystem model. *Ecological Modelling*,  
960 246, 119-130. <https://doi.org/10.1016/j.ecolmodel.2012.06.024>

961 Clark, M. P. et al. (2008). Framework for Understanding Structural Errors (FUSE): A modular  
962 framework to diagnose differences between hydrological models. *Water Resources*  
963 *Research*, 44(12). <https://doi.org/10.1029/2007wr006735>

964 Clark, M. P. et al. (2015a). A unified approach for process-based hydrologic modeling: 1.  
965 Modeling concept. *Water Resources Research*, 51(4), 2498-2514.  
966 <https://doi.org/10.1002/2015WR017198>

967 Clark, M.P. et al. (2015b). A unified approach for process - based hydrologic modeling: 2. Model  
968 implementation and case studies. *Water Resources Research*, 51(4), 2515-2542.  
969 <https://doi.org/10.1002/2015wr017200>

970 Clark, M.P. et al. (2015c). Improving the representation of hydrologic processes in Earth System  
971 Models. *Water Resources Research*, 51(8), 5929-5956.  
972 <https://doi.org/10.1002/2015wr017096>

973 Clark, M. P. et al. (2016). Improving the representation of hydrologic processes in Earth System

974 Models. Water Resources Research, 51(8), 5929-5956.  
975 <https://doi.org/10.1002/2015wr017096>

976 Dai, H. and Ye, M. (2015). Variance-based global sensitivity analysis for multiple scenarios and  
977 models with implementation using sparse grid collocation. *Journal of Hydrology*, 528,  
978 286-300. <https://doi.org/10.1016/j.jhydrol.2015.06.034>

979 Dai, H., Ye, M., Walker, A.P., and Chen, X. (2017a). A new process sensitivity index to identify  
980 important system processes under process model and parametric uncertainty. *Water*  
981 *Resources Research*, 53(4), 3476-3490. <https://doi.org/10.1002/2016wr019715>

982 Dai, H., Chen X., Ye M., Song X., and Zachara, J. M. (2017b). A geostatistics-informed  
983 hierarchical sensitivity analysis method for complex groundwater flow and transport  
984 modeling, *Water Resources Research*, 53, 4327-4343.  
985 <https://doi.org/10.1002/2016WR019756>.

986 Dell'Oca, A., Riva, M., and Guadagnini, A. (2020). Global sensitivity analysis for multiple  
987 interpretive models with uncertain parameters. *Water Resources Research*, 56(2),  
988 e2019WR025754. <https://doi.org/10.1029/2019WR025754>

989 Devak, M., and Dhanya, C.T. (2017). Sensitivity analysis of hydrological models: review and  
990 way forward. *Journal of Water and Climate Change*, 8(4), 557-575.  
991 <https://doi.org/10.2166/wcc.2017.149>

992 Elshall, A. S. and Tsai, F. (2014). Constructive epistemic modeling of groundwater flow with  
993 geological structure and boundary condition uncertainty under the Bayesian paradigm.  
994 *Journal of Hydrology*. 517, 105-119. <https://doi.org/10.1016/j.jhydrol.2014.05.027>

995 Feng, K., Lu, Z., and Yang C. (2019). Enhanced Morris method for global sensitivity analysis:  
996 good proxy of Sobol' index, *Structural and Multidisciplinary Optimization*, 59, 373-387,

997 <https://doi.org/10.1007/s00158-018-2071-7>

998 Gorelick, S. M., Zheng, C., 2015. Global change and the groundwater management challenge.  
999 Water Resources Research, 51(5), 3031-3051. <https://doi.org/10.1002/2014WR016825>

1000 Haan, C. T. (1989). Parametric uncertainty in hydrologic modeling. Transactions of the ASAE,  
1001 32(1), 0137-0146. <https://doi.org/10.13031/2013.30973>

1002 Haghnegahdar, A., Razavi S., Yassin F., and Wheeler H. (2017). Multicriteria sensitivity analysis  
1003 as a diagnostic tool for understanding model behaviour and characterizing model  
1004 uncertainty, Hydrological Processes, 31(25), 4462-4476.  
1005 <https://doi.org/10.1002/hyp.11358>

1006 Herman, J. and Usher, W. (2017) SALib: An open-source Python library for sensitivity analysis.  
1007 Journal of Open Source Software, 2(9). <https://doi.org/10.21105/joss.00097>

1008 Herman, J.D., Reed, P.M. and Wagener, T. (2013). Time-varying sensitivity analysis clarifies the  
1009 effects of watershed model formulation on model behavior. Water Resources Research  
1010 49(3), 1400-1414. <https://doi.org/10.1002/wrcr.20124>

1011 Hock, R. (2003). Temperature index melt modelling in mountain areas. Journal of Hydrology,  
1012 282(1-4), 104-115. [https://doi.org/10.1016/s0022-1694\(03\)00257-9](https://doi.org/10.1016/s0022-1694(03)00257-9)

1013 Huo, X., Gupta, H., Niu, G.-Y., Gong, W. and Duan, Q. (2019) Parameter Sensitivity Analysis  
1014 for Computationally Intensive Spatially Distributed Dynamical Environmental Systems  
1015 Models. Journal of Advances in Modeling Earth Systems 11(9), 2896-2909.  
1016 <https://doi.org/10.1029/2018MS001573>

1017 Ketema, A. A. and Langergraber, G. (2015). Sensitivity analysis of the CLARA Simplified  
1018 Planning Tool using the Morris screening method. Water Science & Technology, 71(2),  
1019 234-244. <https://doi.org/10.2166/wst.2014.497>

1020 Kustas, W. P., Rango, A., and Uijlenhoet, R. (1994). A simple energy budget algorithm for the  
1021 snowmelt runoff model. *Water Resources Research*, 30(5), 1515-1527.  
1022 <https://doi.org/10.1029/94wr00152>

1023 Lu, D., Ye, M., and Curtis, G. P. (2015). Maximum likelihood Bayesian model averaging and its  
1024 predictive analysis for groundwater reactive transport models. *Journal of Hydrology*, 529,  
1025 1859-1873. <https://doi.org/10.1016/j.jhydrol.2015.07.029>

1026 Mai, J., Craig J. R., and Tolson B. A. (2020). Simultaneously determining global sensitivities of  
1027 model parameters and model structure. *Hydrology and Earth System Sciences*, 24, 5835–  
1028 5858. <https://doi.org/10.5194/hess-24-5835-2020>

1029 Markstrom, S.L., Hay, L.E. and Clark, M.P. (2016). Towards simplification of hydrologic  
1030 modeling: identification of dominant processes. *Hydrology and Earth System Sciences*  
1031 20(11), 4655-4671. <https://doi.org/10.5194/hess-20-4655-2016>

1032 Morris, M. D. (1991). Factorial sampling plans for preliminary computational experiments.  
1033 *Technometrics*, 33(2), 161-174. <https://doi.org/10.1080/00401706.1991.10484804>

1034 Neuman, S. P. (2003). Maximum likelihood Bayesian averaging of alternative conceptual-  
1035 mathematical models. *Stochastic Environmental Research and Risk Assessment*, 17(5),  
1036 291-305. <https://doi.org/10.1007/s00477-003-0151-7>

1037 Paleari, L. and Confalonieri, R. (2016). Sensitivity analysis of a sensitivity analysis: We are  
1038 likely overlooking the impact of distributional assumptions. *Ecological Modelling* 340,  
1039 57-63. <https://doi.org/10.1016/j.ecolmodel.2016.09.008>

1040 Pianosi, F. et al. (2016). Sensitivity analysis of environmental models: A systematic review with  
1041 practical workflow. *Environmental Modelling & Software*, 79, 214-232.  
1042 <https://doi.org/10.1016/j.envsoft.2016.02.008>

1043 Poeter, E. P. and Anderson D. A. (2005). Multimodel ranking and inference in ground water  
1044 modeling. *Ground Water*, 43(4), 597-605. <https://doi.org/10.1111/j.1745->  
1045 [6584.2005.0061.x](https://doi.org/10.1111/j.1745-6584.2005.0061.x)

1046 Puy, A., Piano, S. L., and Saltelli, A. (2020). A sensitivity analysis of the PAWN sensitivity  
1047 index. *Environmental Modelling & Software*. *Environmental Modelling & Software*, 127,  
1048 104679. <https://doi.org/10.1016/j.envsoft.2020.104679>

1049 Razavi, S., and Gupta H. V. (2015). What do we mean by sensitivity analysis? The need for  
1050 comprehensive characterization of “global” sensitivity in Earth and Environmental  
1051 systems models. *Water Resources Research*, 51, 3070–3092.  
1052 <https://doi.org/10.1002/2014WR016527>.

1053 Razavi, S. and Gupta, H.V. (2016). A new framework for comprehensive, robust, and efficient  
1054 global sensitivity analysis: 2. Application. *Water Resources Research*, 52, 440–455.  
1055 <https://doi.org/10.1002/2015WR017559>

1056 Razavi, S. et al. (2021). The future of sensitivity analysis: an essential discipline for systems  
1057 modeling and policy support. *Environmental Modelling & Software*, 137, 104954,  
1058 <https://doi.org/10.1016/j.envsoft.2020.104954>

1059 Saltelli, A. et al. (2010). Variance based sensitivity analysis of model output. Design and  
1060 estimator for the total sensitivity index. *Computer Physics Communications*, 181(2), 259-  
1061 270. <https://doi.org/10.1016/j.cpc.2009.09.018>

1062 Saltelli, A., Tarantola S., Campolongo F., and Ratto M. (2004). *Sensitivity Analysis in Practice: A*  
1063 *Guide to Assessing Scientific Models*. John Wiley & Sons, Chichester, England.

1064 Saltelli, A., Ratto, M., Andres, T., Campolongo, F., Cariboni, J., Gatelli, D., Saisana, M., and  
1065 Tarantola, S. (2008). *Global Sensitivity Analysis: the Primer*. Wiley, West Sussex, U. K.

1066 Savage, J.T.S., Pianosi, F., Bates, P., Freer, J. and Wagener, T. (2016). Quantifying the  
1067 importance of spatial resolution and other factors through global sensitivity analysis of a  
1068 flood inundation model. *Water Resources Research* 52(11), 9146-9163.  
1069 <https://doi.org/10.1002/2015WR018198>

1070 Sheikholeslami, R., Gharari, S., Papalexiou, S.M. and Clark, M.P. (2021). VISCOUS: A  
1071 Variance-Based Sensitivity Analysis Using Copulas for Efficient Identification of  
1072 Dominant Hydrological Processes. *Water Resources Research* 57(7), e2020WR028435.  
1073 <https://doi.org/10.1029/2020WR028435>

1074 Singh, V. P. (2018). Hydrologic modeling: progress and future directions. *Geoscience Letters*,  
1075 5(1). <https://doi.org/10.1186/s40562-018-0113-z>

1076 Sobol', I. M., Tarantola, S., Gatelli, D., Kucherenko, S. S., and Mauntz, W. (2007). Estimating  
1077 the approximation error when fixing unessential factors in global sensitivity analysis.  
1078 *Reliability Engineering & System Safety*, 92, 957-960.  
1079 <https://doi.org/10.1016/j.res.2006.07.001>

1080 Song, X., Zhang J., Zhan, C., Xuan, Y., Ye, M., and Xu, C. (2015). Global sensitivity analysis in  
1081 hydrological modeling: Review of concepts, methods, theoretical framework, and  
1082 applications. *Journal of Hydrology*, 523, 739-757.  
1083 <https://doi.org/10.1016/j.jhydrol.2015.02.013>

1084 Van Hoey, S., Seuntjens, P., van der Kwast, J., and Nopens, I. (2014). A qualitative model  
1085 structure sensitivity analysis method to support model selection. *Journal of Hydrology*,  
1086 519: 3426-3435. <https://doi.org/10.1016/j.jhydrol.2014.09.052>

1087 Wainwright, H. M., Finsterle S., Jung Y., Zhou Q., and Birkholzer J. T. (2014). Making sense of  
1088 global sensitivity analysis, *Computers & Geosciences*, 65, 84-94.

1089 <https://doi.org/10.1016/j.cageo.2013.06.006>

1090 Yang, J. (2011). Convergence and uncertainty analyses in Monte-Carlo based sensitivity analysis.

1091 Environmental Modelling & Software 26(4), 444-457.

1092 <https://doi.org/10.1016/j.envsoft.2010.10.007>

1093 Ye, M., Neuman S. P., and Meyer P. D. (2004). Maximum likelihood Bayesian averaging of

1094 spatial variability models in unsaturated fractured tuff. Water Resources Research, 40,

1095 W05113, <https://doi.org/10.1029/2003WR002557>.

1096 Ye, M., Pohlmann, K. F., Chapman, J. B., Pohll, G. M. and Reeves, D. M. (2010). A model-

1097 averaging method for assessing groundwater conceptual model uncertainty. Ground

1098 Water, 48(5): 716-28. <https://doi.org/10.1111/j.1745-6584.2009.00633.x>

1099 Ye, M., Wang L., Pohlmann K. F., and Chapman J.B. (2016). Estimate groundwater interbasin

1100 flow using multiple models and multiple types of calibration data. Ground Water, 54(6),

1101 805-817. <https://doi.org/10.1111/gwat.12422>

1102 Zeng, X. et al. (2018). Identifying key factors of the seawater intrusion model of Dagu river

1103 basin, Jiaozhou Bay. Environmental Research, 165: 425-430.

1104 <https://doi.org/10.1016/j.envres.2017.10.03>

## LIST OF TABLES

**Table 1.** Values of  $\alpha$  and  $a$  of Sobol's  $G^*$ -function used in this study. Ten product elements  $g_i^*$  ( $i = 1, 2, \dots, 10$ ) are considered and each is assumed to represent a process which has two plausible process models,  $g_i^{*1}$  and  $g_i^{*2}$ .

Process	Process model	$\alpha$	$a$	Process	Process model	$\alpha$	$a$
$g_1^*$	$g_1^{*1}$	1	0.002	$g_6^*$	$g_6^{*1}$	1	6.5
	$g_1^{*2}$	2	0.005		$g_6^{*2}$	2	2.3
$g_2^*$	$g_2^{*1}$	1	0.08	$g_7^*$	$g_7^{*1}$	1	10.5
	$g_2^{*2}$	2	0.10		$g_7^{*2}$	2	12
$g_3^*$	$g_3^{*1}$	1	1.5	$g_8^*$	$g_8^{*1}$	1	11
	$g_3^{*2}$	2	1.2		$g_8^{*2}$	2	13
$g_4^*$	$g_4^{*1}$	1	2.1	$g_9^*$	$g_9^{*1}$	1	80
	$g_4^{*2}$	2	2.5		$g_9^{*2}$	2	99
$g_5^*$	$g_5^{*1}$	1	4.2	$g_{10}^*$	$g_{10}^{*1}$	1	85
	$g_5^{*2}$	2	1.8		$g_{10}^{*2}$	2	90

**Table 2.** Analytical  $E_K(d\Delta)$  and  $V_K(d\Delta)$  of parameters under two of 1024 individual system models and those of the three processes considering model uncertainty of the Sobol's  $G^*$ -function.  $S_{Ti}$  denotes Sobol's analytical total-effect sensitivity index, according to which the three processes are ranked from the most non-influential process (numbered by 10) to most influential process (numbered by 1).

Not considering process model uncertainty										
System model	$\prod_{i=1}^{10} g_i^{*1}$									
Parameter	$X_1$	$X_2$	$X_3$	$X_4$	$X_5$	$X_6$	$X_7$	$X_8$	$X_9$	$X_{10}$
$S_{Ti}$ (%)	52.31	46.65	10.63	7.04	2.56	1.24	0.53	0.49	0.011	0.000*
Rank	1	2	3	4	5	6	7	8	9	10
$E_K(d\Delta)$ ( $\times 10^{-2}$ )	66.53	61.76	26.67	21.51	12.82	8.89	5.80	5.56	0.823	0.775
$V_K(d\Delta)$ ( $\times 10^{-2}$ )	50.96	46.81	12.23	8.18	3.01	1.46	0.62	0.57	0.013	0.011
System model	$\prod_{i=1}^{10} g_i^{*2}$									
Parameter	$X_1$	$X_2$	$X_3$	$X_4$	$X_5$	$X_6$	$X_7$	$X_8$	$X_9$	$X_{10}$
$S_{Ti}$ (%)	57.16	51.47	18.34	7.93	11.97	8.85	0.61	0.53	0.010	0.012
Rank	1	2	3	6	4	5	7	8	10	9
$E_K(d\Delta)$ ( $\times 10^{-2}$ )	99.50	90.91	45.45	28.57	35.71	30.30	7.69	7.14	1.00	1.10
$V_K(d\Delta)$ ( $\times 10^{-2}$ )	290.92	268.49	104.48	45.92	68.93	51.19	3.56	3.76	0.06	0.07
Considering process model uncertainty										
Process	$g_1^*$	$g_2^*$	$g_3^*$	$g_4^*$	$g_5^*$	$g_6^*$	$g_7^*$	$g_8^*$	$g_9^*$	$g_{10}^*$
$E_K(d\Delta)$ ( $\times 10^{-2}$ )	102.64	96.82	37.28	26.75	26.38	21.75	6.92	6.43	0.921	0.954
$V_K(d\Delta)$ ( $\times 10^{-2}$ )	108.17	96.96	44.58	21.10	25.14	17.93	1.67	1.48	0.030	0.033

\* This value is rounded to zero.

**Table 3.** Numerical  $E_K(d\Delta)$  and  $V_K(d\Delta)$  of parameters under individual system model and those of the three processes considering model uncertainty of the groundwater flow model using LHS with  $n = 5000$ .  $S_{Ti}$  denotes Sobol's total-effect sensitivity index calculated numerically by using  $10,000 \times (k + 2)$  simulation runs, where  $k$  is the number of parameters in the system model. Without considering process model uncertainty, the three processes are ranked according to  $S_{Ti}$  for each of the eight individual system models. With considering process model uncertainty, the three processes are ranked according to the  $E_K(d\Delta)$  and  $V_K(d\Delta)$  values. Note the most non-influential process is numbered by 3 while the most influential process is numbered by 1.

Not considering process model uncertainty												
Model	$R_1G_1M_1$			$R_1G_1M_2$			$R_1G_2M_1$			$R_1G_2M_2$		
Parameter	$a$	$K$	$fl$	$a$	$K$	$f_2\&r$	$a$	$K_1\&K_2$	$fl$	$a$	$K_1\&K_2$	$f_2\&r$
$S_{Ti}$ (%)	12.37	36.87	66.06	14.98	55.74	37.95	34.08	15.78	54.65	35.83	38.66	27.97
Rank	3	2	1	3	1	2	2	3	1	2	1	3
$E_K(d\Delta)$ ( $\times 10^{-2}$ )	42.61	56.00	85.80	42.61	69.90	60.01	53.40	34.62	65.96	53.40	54.43	46.14
$V_K(d\Delta)$ ( $\times 10^{-2}$ )	10.37	53.10	76.23	10.37	57.51	36.92	17.08	8.49	29.67	17.08	19.47	14.38
Model	$R_2G_1M_1$			$R_2G_1M_2$			$R_2G_2M_1$			$R_2G_2M_2$		
Parameter	$b$	$K$	$fl$	$b$	$K$	$f_2\&r$	$b$	$K_1\&K_2$	$fl$	$b$	$K_1\&K_2$	$f_2\&r$
$S_{Ti}$ (%)	22.04	32.82	58.80	26.02	48.49	33.01	49.55	14.43	39.79	50.30	32.16	19.67
Rank	3	2	1	3	1	2	1	3	2	1	2	3
$E_K(d\Delta)$ ( $\times 10^{-2}$ )	61.66	56.00	85.80	61.66	69.90	60.01	77.27	38.65	65.96	77.27	59.04	46.14
$V_K(d\Delta)$ ( $\times 10^{-2}$ )	19.01	53.10	76.23	19.01	57.51	36.92	31.44	10.82	29.67	31.44	23.20	14.38
Considering process model uncertainty												
Process	Recharge			Geology			Snowmelt					
Rank	3			2			1					
$E_K(d\Delta)$ ( $\times 10^{-2}$ )	61.93			66.19			130.11					
$V_K(d\Delta)$ ( $\times 10^{-2}$ )	21.96			43.25			146.93					

## LIST OF FIGURES

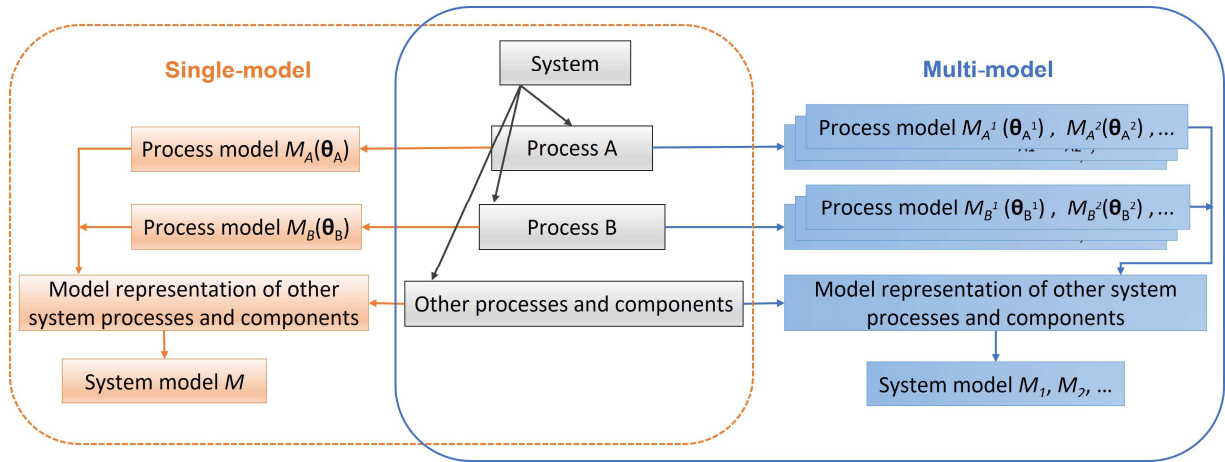


**Fig. 1.** Relation between a system and its processes as well as relation between a system model and process models. The left box represents the conventional single-model framework, in which each process is represented by only one process model and only one system model is formulated. The right box represents the multi-model framework, in which each process can be represented by multiple alternative process models and multiple alternative system models are formulated.

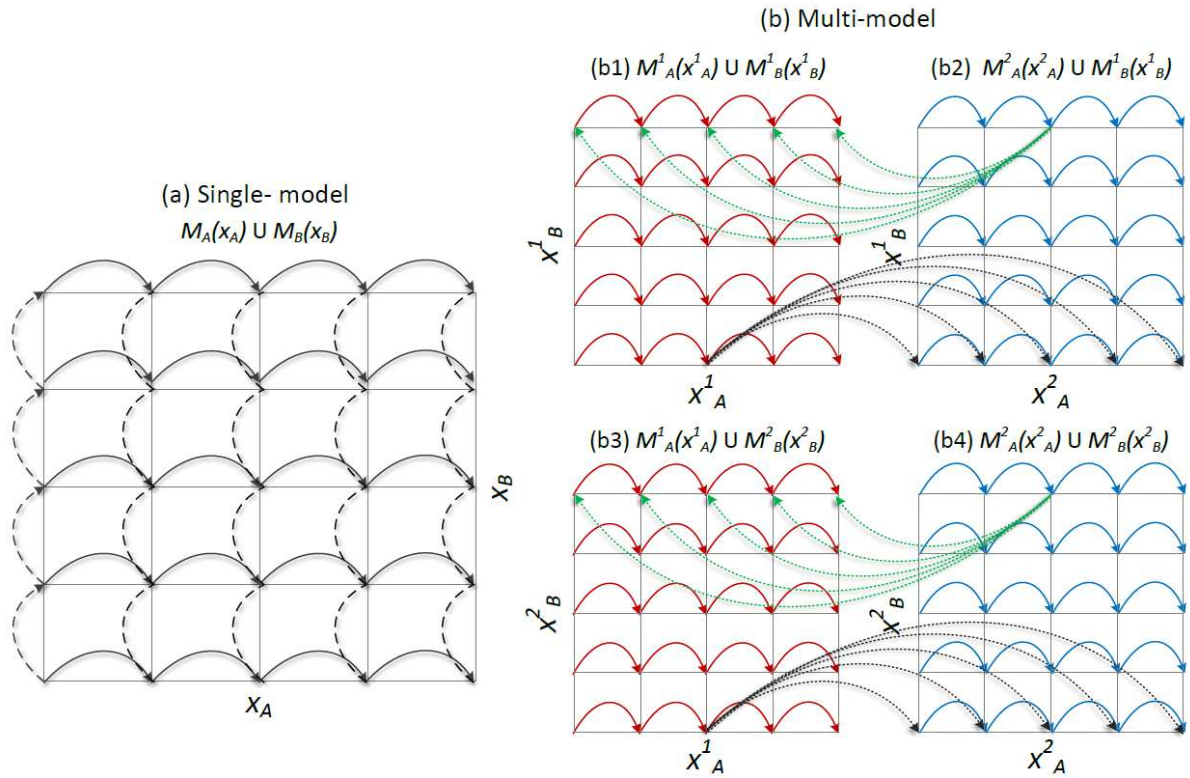


**Fig. 2.** (a) Illustration of Morris method for a single system model containing two processes  $A$  and  $B$ , which are represented by process models  $M_A$  and  $M_B$ , respectively. Each model has its one parameter,  $x_A$  for  $M_A$  and  $x_B$  for  $M_B$ . The horizontal solid arrows represent 20 elementary effects related to  $x_A$ , and the vertical dashed arrows represent 20 elementary effects related to  $x_B$ . (b) Illustration of MMADS with multiple process models. Process  $A$  is represented by two alternative process models,  $M_A^1$  and  $M_A^2$ , with parameters  $x_A^1$  and  $x_A^2$ , respectively. Process  $B$  is represented by two alternative process models  $M_B^1$  and  $M_B^2$ , with parameter  $x_B^1$  and  $x_B^2$ , respectively. The red and blue solid arrows indicate that parameter values vary within a process model. The green and black dotted arrows indicate a transition from one to the other process model and a transition of parameter value from one to the other process model.

```

Use LHS method to generate the sampling matrix of all uncertainty parameters
Loop [1] over process model combinations  $M_{\sim K}$  for process  $\sim K$  in  $\mathbf{M}_{\sim K}$ 
  Combine parameter values for parameters associate with  $M_{\sim K}$  to yield  $\boldsymbol{\theta}_{\sim K} | M_{\sim K}$ 
  Loop [2] over parameter realizations  $\boldsymbol{\theta}_{\sim K} | M_{\sim K}$ 
    Loop [3] over process models  $M_K$  for process  $K$  in  $\mathbf{M}_K$ 
      Combine parameter values for parameters associated with  $M_K$  to yield  $\boldsymbol{\theta}_K | M_K$ 
      Loop [4] over parameter realizations  $\boldsymbol{\theta}_K | M_K$ 
        Compute  $\Delta | \boldsymbol{\theta}_{\sim K}, M_{\sim K}, \boldsymbol{\theta}_K, M_K$ 
      End loop [4]
    End loop [3]
  Loop [5] over process model transitions in  $T_{\mathbf{M}_K}$ 
    Loop [6] over parameter realizations  $T_{\boldsymbol{\theta}_K | T_{\mathbf{M}_K}}$  associated with  $T_{\mathbf{M}_K}$ 
      Compute  $d\Delta | \boldsymbol{\theta}_{\sim K}, M_{\sim K}, T_{\boldsymbol{\theta}_K}, T_{M_K}$  and  $(d\Delta | \boldsymbol{\theta}_{\sim K}, M_{\sim K}, T_{\boldsymbol{\theta}_K}, T_{M_K})^2$ 
    End Loop [6]
    Compute  $E_{T_{\boldsymbol{\theta}_K | T_{\mathbf{M}_K}}} (d\Delta | \boldsymbol{\theta}_{\sim K}, M_{\sim K}, T_{\boldsymbol{\theta}_K}, T_{M_K})$  and  $E_{T_{\boldsymbol{\theta}_K | T_{\mathbf{M}_K}}} (d\Delta | \boldsymbol{\theta}_{\sim K}, M_{\sim K}, T_{\boldsymbol{\theta}_K}, T_{M_K})^2$ 
  End Loop [5]
  Compute  $E_{T_{\mathbf{M}_K}} E_{T_{\boldsymbol{\theta}_K | T_{\mathbf{M}_K}}} (d\Delta | \boldsymbol{\theta}_{\sim K}, M_{\sim K}, T_{\boldsymbol{\theta}_K}, T_{M_K})$  and
   $E_{T_{\mathbf{M}_K}} E_{T_{\boldsymbol{\theta}_K | T_{\mathbf{M}_K}}} (d\Delta | \boldsymbol{\theta}_{\sim K}, M_{\sim K}, T_{\boldsymbol{\theta}_K}, T_{M_K})^2$  using model averaging
End Loop [2]
Compute  $E_{\boldsymbol{\theta}_{\sim K} | M_{\sim K}} E_{T_{\mathbf{M}_K}} E_{T_{\boldsymbol{\theta}_K | T_{\mathbf{M}_K}}} (d\Delta | \boldsymbol{\theta}_{\sim K}, M_{\sim K}, T_{\boldsymbol{\theta}_K}, T_{M_K})$  and
 $E_{\boldsymbol{\theta}_{\sim K} | M_{\sim K}} E_{T_{\mathbf{M}_K}} E_{T_{\boldsymbol{\theta}_K | T_{\mathbf{M}_K}}} (d\Delta | \boldsymbol{\theta}_{\sim K}, M_{\sim K}, T_{\boldsymbol{\theta}_K}, T_{M_K})^2$ 
End Loop [1]
Compute  $E_{\mathbf{M}_{\sim K}} E_{\boldsymbol{\theta}_{\sim K} | M_{\sim K}} E_{T_{\mathbf{M}_K}} E_{T_{\boldsymbol{\theta}_K | T_{\mathbf{M}_K}}} (d\Delta | \boldsymbol{\theta}_{\sim K}, M_{\sim K}, T_{\boldsymbol{\theta}_K}, T_{M_K})$  and
 $E_{\mathbf{M}_{\sim K}} E_{\boldsymbol{\theta}_{\sim K} | M_{\sim K}} E_{T_{\mathbf{M}_K}} E_{T_{\boldsymbol{\theta}_K | T_{\mathbf{M}_K}}} (d\Delta | \boldsymbol{\theta}_{\sim K}, M_{\sim K}, T_{\boldsymbol{\theta}_K}, T_{M_K})^2$  using model averaging

```

**Fig. 3.** Pseudo code for evaluating  $E_K(d\Delta)$  and  $V_K(d\Delta)$  defined in Eqs. (4) and (5) for process  $K$ .

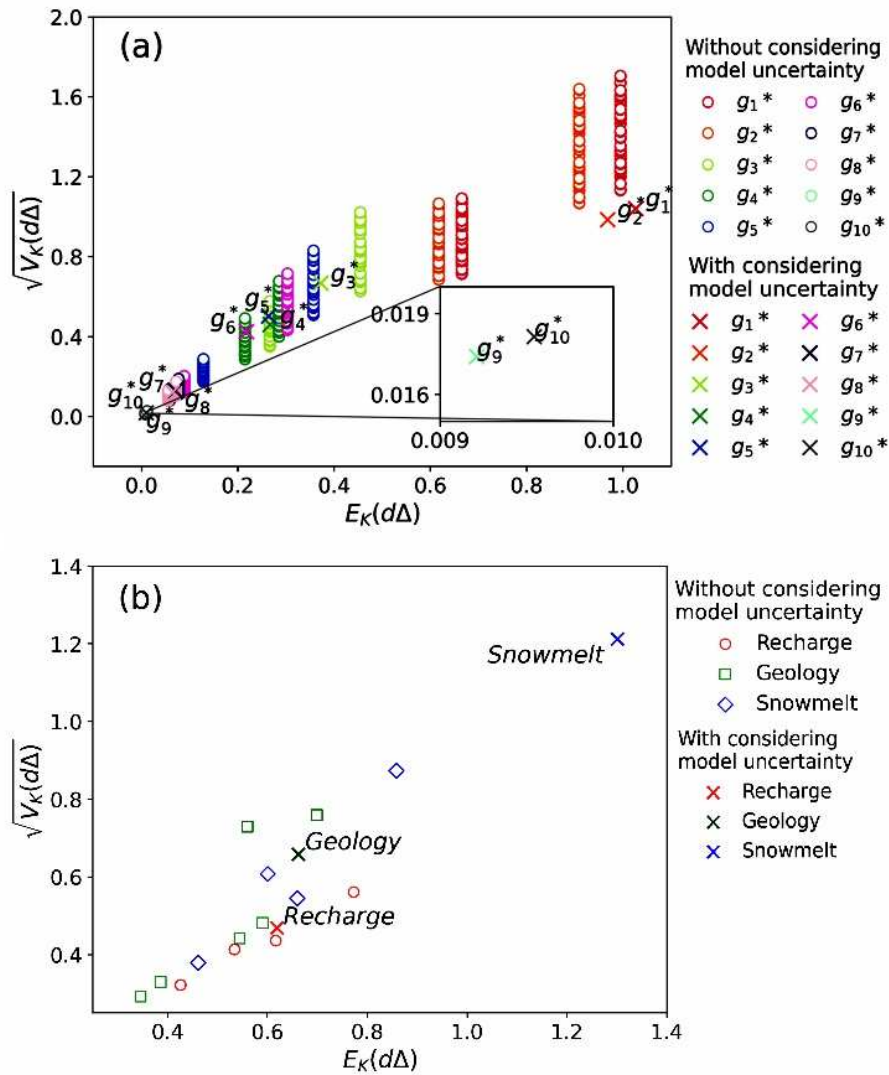


**Fig. 4.** Plots of  $E_K(d\Delta)$  and  $\sqrt{V_K(d\Delta)}$  for the processes of (a) the Sobol's  $G^*$ -function and (b) the groundwater flow modeling. The ten processes of Sobol's  $G^*$ -function and the three processes of groundwater flow modeling are marked with different colors. Open symbols are for individual system models that only consider parametric uncertainty. Cross symbols denote the sensitivity measures with a consideration of uncertainty in process models and parameters.

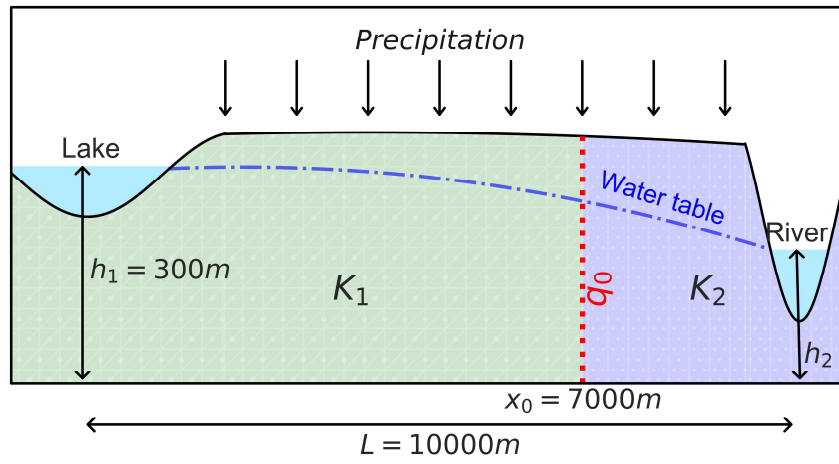


**Fig. 5.** Sketch of one-dimensional groundwater flow model.

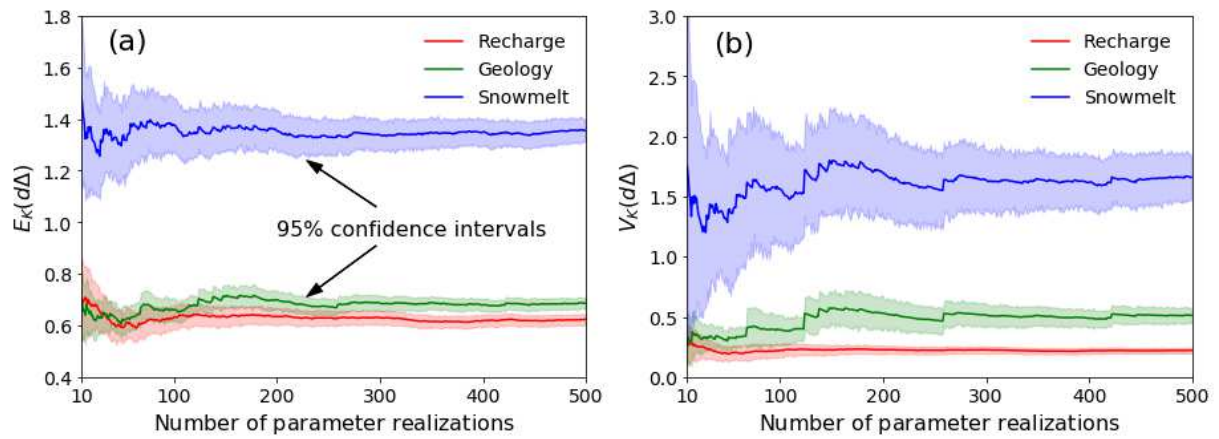


**Fig. 6.** Convergence of (a)  $E(d\Delta)$  and (b)  $V(d\Delta)$  of the three processes of groundwater flow modeling. The areas are for the 95% confidence intervals estimated using bootstrapping with 100 samples.

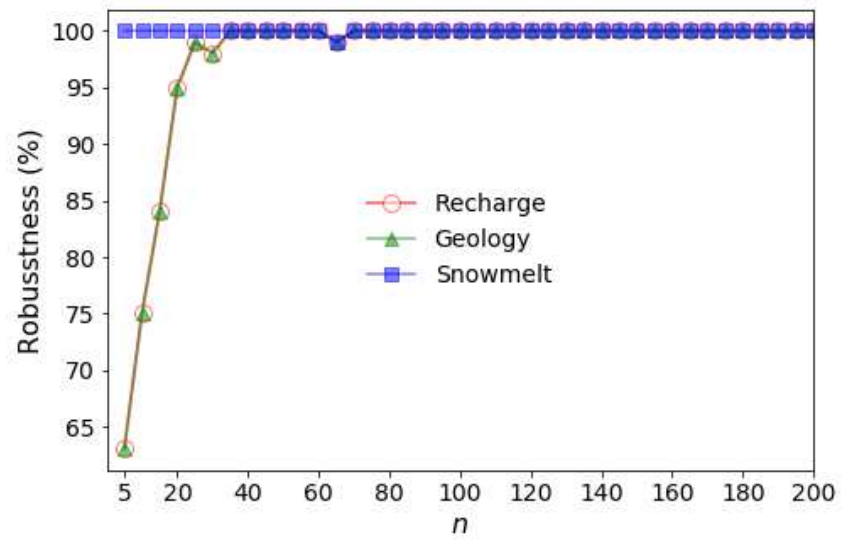


**Fig. 7.** Assessment of MMADS robustness based on process ranking in the example of groundwater flow modeling. The number,  $n$ , of parameter samples used in LHS sampling increases gradually from 5 to 200.

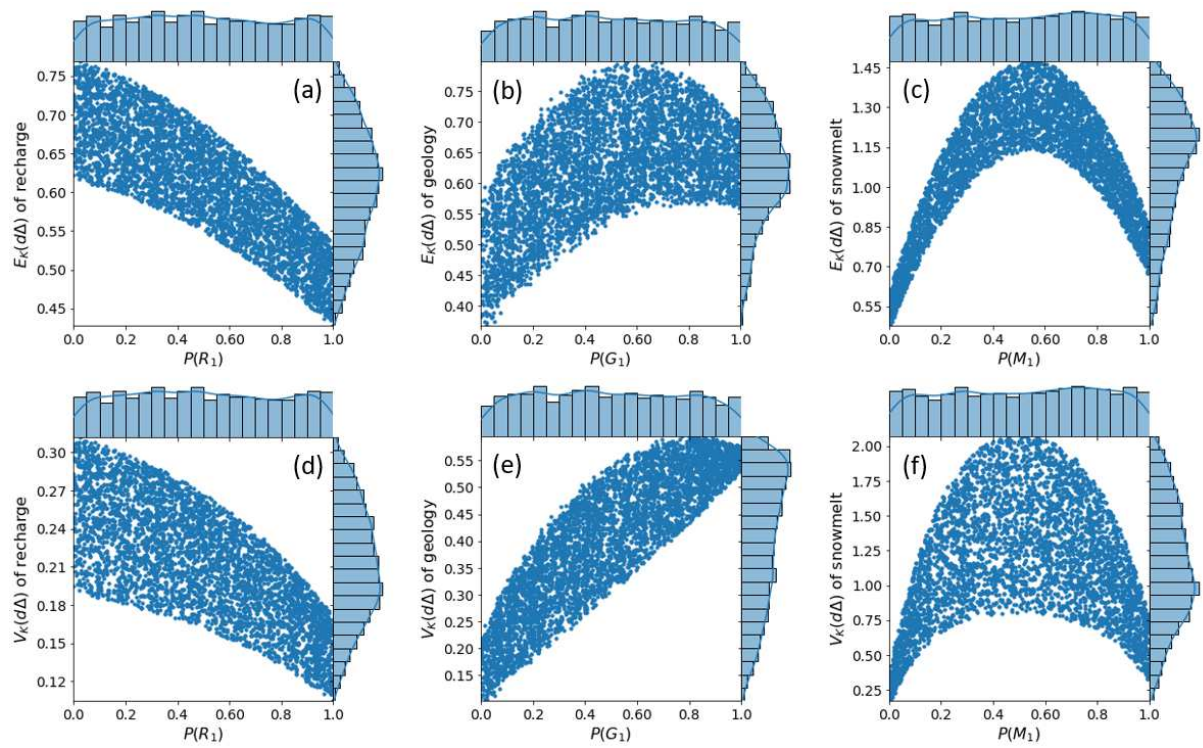


**Fig. 8.** Variation of  $E_K(d\Delta)$  and  $V_K(d\Delta)$  for the three groundwater processes with process model probabilities. Variations of (a)  $E_K(d\Delta)$  and (d)  $V_K(d\Delta)$  of recharge process with  $P(R_1)$ , (b)  $E_K(d\Delta)$  and (e)  $V_K(d\Delta)$  of geology process with  $P(G_1)$ , and (c)  $E_K(d\Delta)$  and (f)  $V_K(d\Delta)$  of snowmelt process with  $P(M_1)$ .

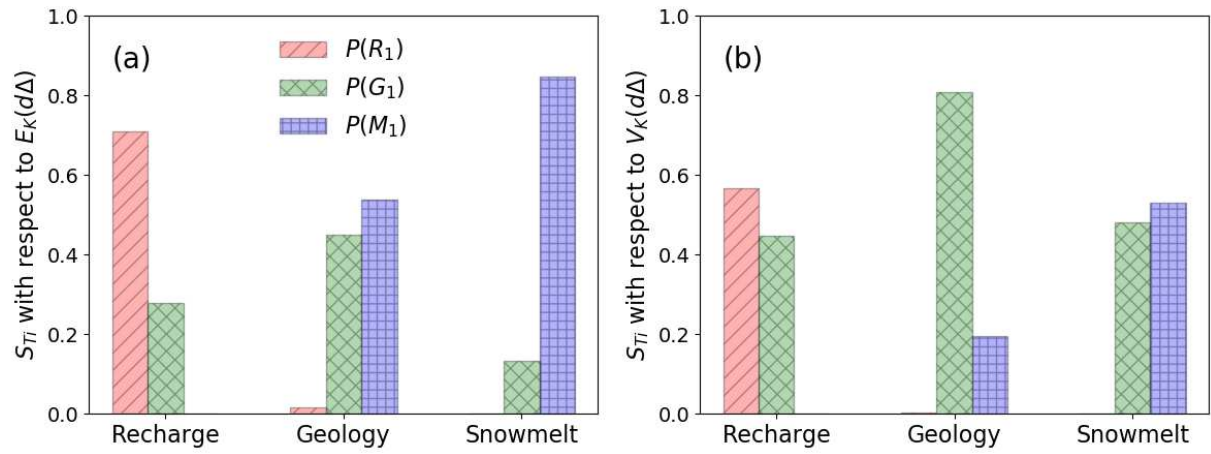


**Fig. 9.** Sobol's total-effect sensitivity indices ( $S_{Ti}$ ) evaluated to measure sensitivity of (a)  $E_K(d\Delta)$  and (b)  $V_K(d\Delta)$  of the three groundwater flow processes to for process model probabilities,  $P(R_1)$ ,  $P(G_1)$ , and  $P(M_1)$ .